Atomic structure, alloying behavior, and magnetism in small Fe-Pt clusters

Bheema Lingam Chittari[1,*] and Vijay Kumar[1,2,†]
[1]*Dr. Vijay Kumar Foundation, 1969 Sector 4, Gurgaon 122001, Haryana, India*
[2]*Center for Informatics, School of Natural Sciences, Shiv Nadar University, NH91, Tehsil Dadri, Gautam Budhha Nagar 201314, U.P., India*

(Received 8 October 2014; revised manuscript received 11 March 2015; published 30 September 2015)

We report results of the atomic structure, alloying behavior, and magnetism in Fe_mPt_n ($m+n=2$–10) clusters using projector augmented wave (PAW) pseudopotential method and spin-polarized generalized gradient approximation (GGA) for the exchange-correlation energy. These results are compared with those obtained by using HCTH exchange-correlation functional and LANL2DZ basis set in the Gaussian program and the overall trends are found to be similar. As in bulk Fe-Pt alloys, clusters with equal composition of Fe and Pt have the largest binding energy and the largest heat of nanoalloy formation for a given number of atoms in the cluster. There are some deviations due to the different symmetries in clusters and in cases where the total number of atoms is odd. The lowest energy isomers tend to maximize bonds between unlike atoms with Fe (Pt) atoms occupying high (low) coordination sites in the core (surface) of the cluster. The binding energy, heat of formation, and the second order difference of the total energy show Fe_2Pt_2, Fe_4Pt_4, and Fe_4Pt_6 clusters to be the most stable ones among the different clusters we have studied. The magnetic moments on Fe atoms are *high* in Pt-rich clusters as well as in small Fe-rich clusters and decrease as the aggregation of Fe atoms and the cluster size increases. The maximum value of the magnetic moments on Fe atoms is $\sim$3.8 μ_B, whereas for Pt atoms it is 1 μ_B. These are quite high compared with the values for bulk Fe as well as bulk FePt and Fe_3Pt phases while bulk Pt is nonmagnetic. There is significant charge transfer from those Fe atoms that interact directly with Pt atoms. We discuss the hybridization between the electronic states of Pt and Fe atoms as well as the variation in the magnetic moments on Fe and Pt atoms. Our results provide insight into the understanding of the nanoalloy behavior of Fe-Pt and we hope that this would help to design Fe based nanoalloys and their assemblies with high magnetic moments for strong magnets without rare earths as well as Pt alloy catalysts.

DOI: 10.1103/PhysRevB.92.125442 PACS number(s): 36.40.Cg, 75.50.Bb, 73.22.Dj, 75.75.Lf

I. INTRODUCTION

Nanostructures of Fe-Pt alloys have attracted much interest due to their applications in ultrahigh density magnetic recording media [1–6] as well as in catalysis [7]. This is due to the fact that bulk FePt alloy has high magnetic crystalline anisotropy (MCA) and coercivity with $L1_0$ structure [8]. However, FePt nanoparticles have been reported to have ordered $L1_0$ structure only in the size range of greater than 2.5 nm [8,9]. Below this size the nanoparticles tend to have disordered structures. This small size region is important from a catalysis point of view. Small clusters of elemental Pt have much higher reactivity [10] compared to larger nanoparticles and it is of interest to know the effects of alloying on their properties. There are experiments [7] that show much higher catalytic activity on Pt nanoparticles alloyed with Fe and other elements or in the form of core shell nanoparticles of Pt as compared to that of the pure Pt nanoparticles. Therefore, an understanding of the atomic structure and alloying behavior of small nanoparticles or clusters of Fe-Pt is very desirable.

Recently, a few selected small clusters, namely FePt, Fe_2Pt_2, Fe_3Pt_3, Fe_4Pt_4, and Fe_5Pt_5 with equal numbers of Fe and Pt atoms, have been studied with and without spin-orbit coupling [11]. The ground state isomers of these clusters have maximum Fe-Pt bonds and large binding energy (BE). Notably, the spin-orbit interaction has been found to have very little effect on the magnetic moments in clusters beyond a dimer. In particular, the magnetic moments on a Fe atom are enhanced by 4.6% and on a Pt atom by 30% when spin-orbit interaction is included in the FePt dimer, but the enhancement in the magnetic moments is by only 0.29% for Fe atoms and 5% for Pt atoms when the cluster size is increased to Fe_2Pt_2. Also, the average orbital magnetic moment of Fe in the FePt dimer is high but it vanishes with the size of the cluster [11]. Accordingly, the contribution of spin-orbit coupling as well as orbital magnetic moment is significant only for very small clusters. Here we study Fe-Pt clusters having a total of up to ten atoms with varying numbers of Fe and Pt atoms and neglect the contributions from spin-orbit coupling as well as orbital magnetic moment. We study the ordering behavior in these nanoalloys and calculate the BE as well as the heat of formation (ΔH) to identify the most stable clusters in this size range and to understand the variation in the magnetic moments. While in bulk, FePt phase is the most stable one, in nanoalloys the most stable clusters may not necessarily have equal concentrations of Fe and Pt as the atomic structure of clusters (often different from bulk) also plays an important role. We have also explored different spin isomers to find the lowest energy structures and to understand the magnetic behavior.

It is instructive to mention that the atomic radius of Pt is larger than the value for a Fe atom and the surface energy of Pt is lower than that of Fe [12]. It has been shown that the larger atom or the element with lower surface energy tends to segregate on alloy surfaces [13]. As clusters have a large

*Present address: SKKU Advanced Institute of Nano-Technology (SAINT), Sung Kyun Kwan University, Suwon 440-746, Republic of Korea.
†Corresponding author: kumar@vkf.in; vijay.kumar@snu.edu.in

 ©2015 American Physical Society

fraction of atoms on the surface, we expect in nanoalloys of Fe-Pt a tendency for Pt enrichment on the surface. The surface segregation is generally significantly affected in ordering alloys such as bulk Fe-Pt as well as in alloys with positive ΔH. The experimental ΔH in bulk Fe-Pt alloys is negative and is the highest for bulk FePt among the three ordered phases $FePt_3$, FePt, and Fe_3Pt [14]. A natural question is then how the ordering and segregation behavior would be affected by the finite size in Fe-Pt clusters. Moreover, small Pt clusters favor relatively open structures [15] and in many cases these are planar. On the other hand, Fe clusters have close packed structures [16]. Therefore, the question is how the atomic structures and properties will get affected by alloying of Fe and Pt in small sizes. Furthermore, very interestingly in Fe-Pt bulk alloys, the addition of Pt to Fe increases significantly the magnetic moment on Fe atoms. In addition, when one goes from bulk Fe to clusters, the magnetic moments on Fe atoms tend to increase. It has been shown that small Fe clusters have a large magnetic moment of about 3 μ_B/atom [17]. In Fe-Pt nanoalloys, different structures, charge transfer, and hybridization between Fe and Pt electronic states could further affect the magnetic moments. All these considerations make the study of small Fe-Pt clusters interesting and the resulting variations in the magnetic behavior as well as other physical and chemical properties could provide insight for understanding magnetism and atomic distribution in larger clusters. We explore here small Fe_mPt_n ($m + n = 2$–10) clusters over the whole range of compositions to understand the evolution of the atomic and electronic structure as well as the magnetic and charge transfer behavior along with ΔH, BE, and the second order difference (Δ_2) of the total energy. Our results demonstrate high magnetic moments on Fe atoms in Pt-rich as well as small Fe-rich clusters and the preference of Pt atoms to occupy low coordination sites. There is also significant charge transfer from Fe atoms to nearest Pt atoms.

In the following section we discuss our method of calculations while in Sec. III we present our results. Our conclusions are given in Sec. IV.

II. METHOD OF CALCULATION

The calculations have been performed within the framework of the density functional theory [18] using the Vienna *ab initio* simulation package (VASP) [19,20]. We considered 14 valence electrons (including the 3p semicore electrons) for Fe and 10 valence electrons for Pt atoms. The electron-ion interactions have been treated using pseudopotentials within the projector augmented wave [21,22] method. The valence electron wave functions have been expanded in terms of a plane-wave basis set using medium precision in VASP code. We used spin-polarized generalized gradient approximation for the exchange-correlation functional following the formulation of Perdew, Burke, and Ernzerhof (PBE) [23]. The clusters were placed in a cubic supercell with an edge length of 15 Å to avoid interactions between the periodic images. The Brillouin zone is represented by the Γ point. The atomic structures of elemental Pt clusters are considered from earlier work [15], whereas for Fe we have considered several initial choices of the atomic structures and the optimized lowest energy structures are in good agreement with recent studies [16].

We generated the initial structures of Fe-Pt clusters from the knowledge of the atomic structures of small clusters of pure Fe (Pt) by replacing some of the Fe (Pt) atoms with Pt (Fe) atoms. Also, few structures have been constructed by adding atoms on the converged structures of smaller clusters or by removal of atoms from larger clusters. Additionally, low lying atomic structures known in literature for some metal clusters have been explored. The atomic structure relaxations have been performed without using any constraints. Furthermore, we explored spin isomers and optimized the atomic structures again to obtain the lowest energy structures that generally have ferromagnetic coupling. The structural relaxation has been performed by using the conjugate gradient method. The convergence criterion for the force on each ion is taken to be less than 0.005 eV/Å. The magnetic moments and charge on each atom have been calculated from Bader charge analysis. The experimental bond length of Fe_2 is 2.02 ± 0.02 Å [24], the BE is 0.57 eV/atom [25], and the vibrational frequency is 299.6 cm^{-1} [26]. However, the calculated BE of Fe_2 is 1.6 eV/atom using PBE functional which is much larger than the experimental value. Therefore, we performed calculations with PBE0 [27] and HSE06 [28] functional in VASP. The ground state of Fe_2 is found to have 8 μ_B magnetic moments using PBE0 and HSE06 functional unlike in the case of PBE functional that the ground state has 6 μ_B magnetic moments. Furthermore, as compared to PBE, the BE is found to be higher, i.e., 2.25 and 1.96 eV/atom using PBE0 and HSE06, respectively, with 6 μ_B. However, the calculated bond length of Fe_2 with 6 μ_B magnetic moments is 2.006, 2.265, and 2.250 Å using PBE, PBE0, and HSE06 functional, respectively. It is contingent from these VASP calculations that the results obtained using PBE are in better agreement with experiments compared to PBE0. There have been also efforts to study the effects of including Hubbard U with PBE calculations [29,30]. We have also considered Fe-rich isomers of Fe-Pt clusters (namely Fe_3Pt and Fe_4Pt) for understanding the ground state structures as obtained with PBE as well as with PBE0 functional for different fixed spin multiplicities. Unlike Fe_2, we have found that in these cases the ground state in PBE0 has the same magnetic moment as with PBE. However, the Fe-Fe bond lengths are found to be elongated by about 8% for Fe_3Pt and 5% for Fe_4Pt using PBE0 compared to PBE. A recent study [31] on bulk Fe also reveals large BE and large lattice parameter with HSE06 functional compared to the PBE functional. Therefore, we further performed a calculation on Fe dimer using the GAUSSIAN09 program [32] with the semiempirical Hamprecht, Cohen, Tozer, and Handy (HCTH) exchange-correlation functional [33–35] along with Los Alamos National Laboratory effective core potentials and LANL2DZ basis set [36–38]. The optimized bond length is 2.042 Å, which is in good agreement with the experimental value [24] and the BE is found to be 1.10 eV/atom. Also we performed an all electron calculation using the GAUSSIAN09 program with 6-311+g* basis set and PBE0 functional and obtained 1.031 eV for the BE of Fe_2 and the frequency to be 311 cm^{-1}. This is in good agreement with the experimental value. As the values of the BE and bond length obtained by using HCTH/LANL2DZ are closer to the experimental values compared to those obtained with PBE, PBE0, and HSE06 functional in VASP (see Table S1 and Fig. S1 in the

Supplemental Material [39] for comparison of results obtained from various methods of calculations along with the experimental values), we have compared all the results obtained with PBE in VASP with the calculations using HCTH/LANL2DZ in the Gaussian program. However, it is found that the trends in the BE, ΔH, Δ_2, and the magnetic moments are similar and the structures obtained from PBE remain almost the same using HCTH/LANL2DZ. The overestimation of the BE using PBE leads to an almost rigid shift of the BE curve compared to the one obtained with HCTH/LANL2DZ. The dynamical stability of the clusters is further studied by calculating infrared (IR) and Raman spectra for the lowest energy isomers.

III. RESULTS

We discuss the atomic structures and magnetic moments on different clusters in the following subsections. The BE, dipole moment (D), Δ_2, and ΔH values for Fe_mPt_n ($m+n=2$–10) clusters calculated from PBE in VASP and HCTH/LANL2DZ in the GAUSSIAN09 program are listed in Tables S2 and S3 in the Supplemental Material [39] along with the values for the pure Fe and Pt clusters. The lowest energy structures for different compositions of clusters with up to ten atoms along with numbering of atoms are given in Table S4 in the Supplemental Material [39]. Also the magnetic moments on each atom in different clusters are given in Tables S5–S9 in the Supplemental Material [39].

A. Fe_N and Pt_N (N = 2–10) clusters

As a first step, we optimized pure Fe_N and Pt_N ($N=2$–10) clusters. In this size range, Pt clusters generally prefer open structures [15,16] but Fe clusters have close packed structures as shown in Fig. 1. For $N=2$ and 3, the atomic structures of Fe and Pt clusters are similar, but Pt_4 has a bent rhombus structure, whereas Fe_4 is a tetrahedron. For $N=5$, a side capped slightly distorted square has the lowest energy for Pt, but a trigonal bipyramid has the lowest energy for Fe_5. Pt_6 has a two-dimensional (2D) triangular structure while Fe_6 is an octahedron. Pt_7 has a side capped slightly distorted double square structure, but a pentagonal bipyramid is the lowest in energy for Fe_7. For Pt_8 a bicapped Pt_6 cluster with an atom capping on both sides of the central triangle has the lowest energy, but Fe_8 is stabilized as bicapped trigonal prism (8a). A side bicapped octahedron (8b) is nearly degenerate. Pt_9 has a planar structure with four squares, whereas Fe_9 has a bicapped centered hexagon (9a) structure and a tricapped trigonal prism (9b) is only 0.07 eV higher in energy. Pt_{10} is the most stable structure with a tetracapped octahedron (10a) which is also a tetrahedron, whereas a bicapped tetragonal antiprism is the lowest in energy for Fe_{10}. Note that a tetracapped trigonal prism (10b) derived from (9b) by adding an atom on the top is nearly degenerate with only 0.06 eV higher energy. Another isomer (10c) with two perpendicularly fused pentagonal bipyramids lies only 0.28 eV higher in energy. For Fe clusters our results agree with those obtained earlier [16]. The BE of Fe and Pt clusters obtained by using PBE in VASP and HCTH/LANL2DZ in the GAUSSIAN09 program are compared in Fig. S1 in the Supplemental Material [39]. Among the Pt clusters, Pt_{10} has 8 μ_B magnetic moments in a tetrahedral structure, while Pt_3 and Pt_6 have 0 μ_B magnetic moment in planar structures. The zero magnetic moment is due to ferromagnetic as well as antiferromagnetic coupling between the spins on neighboring atoms in these clusters [15]. Pt_4 and Pt_7 have 4 μ_B, while the rest of the clusters have 2 μ_B magnetic moments. The magnetic moments on Fe clusters, however, increase with increasing size due to the ferromagnetic coupling between the spins. Recent x-ray magnetic circular dichroism experiments on total magnetic moments suggest that small iron clusters have 3.2–3.9 μ_B/atom [40], whereas our calculated values range from 2.8 to 3.6 μ_B/atom. The variation in the magnetic moments from experiments is also due to the fact that the experiments were done on charged iron clusters (Fe_N^+) and that some contribution may come from orbital magnetic moments.

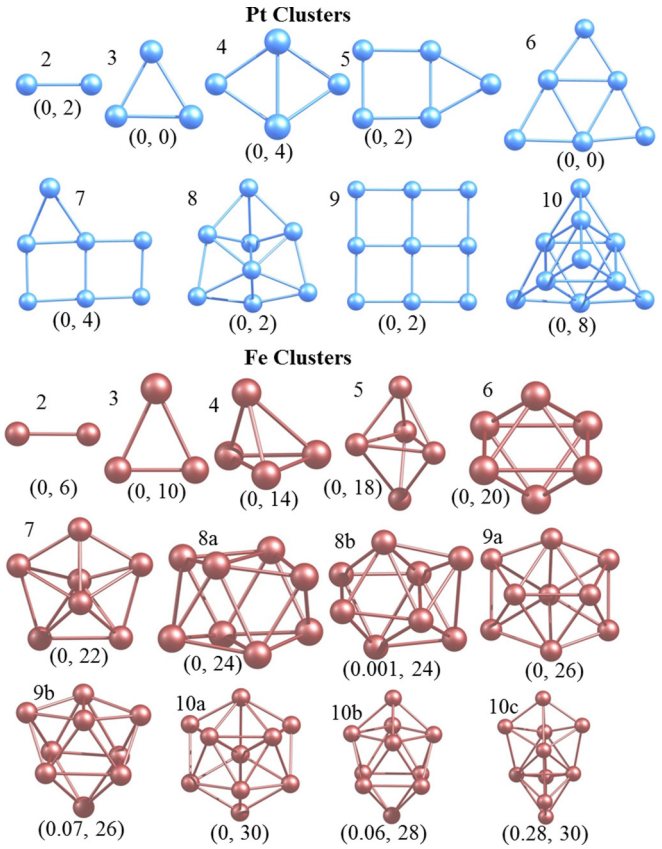

FIG. 1. (Color online) Low lying isomers of Pt_N and Fe_N clusters with $N=2$–10. Na, Nb, ... are isomers with increasing order of energy. The numbers in brackets refer to the energy (eV) relative to the lowest energy isomer and the magnetic moment (μ_B).

We conclude this section with the note that small Pt clusters have relatively open structures and small magnetic moments, while Fe clusters have compact structures and large magnetic moments of $\geqslant 3\,\mu_B$/atom except for $N=9$ for which it is just slightly less than 3 μ_B/atom. It is of interest to find out how the atomic structure and properties evolve as we mix Fe and Pt to develop nanoalloys. By mixing, the moments can change due to the charge transfer from Fe to Pt as well as by hybridization between the Fe and Pt states. In the following we present results on Fe-Pt clusters with varying number of Fe and Pt atoms and discuss the trends in the values of ΔH, evolution of the atomic structure, and the magnetic moments.

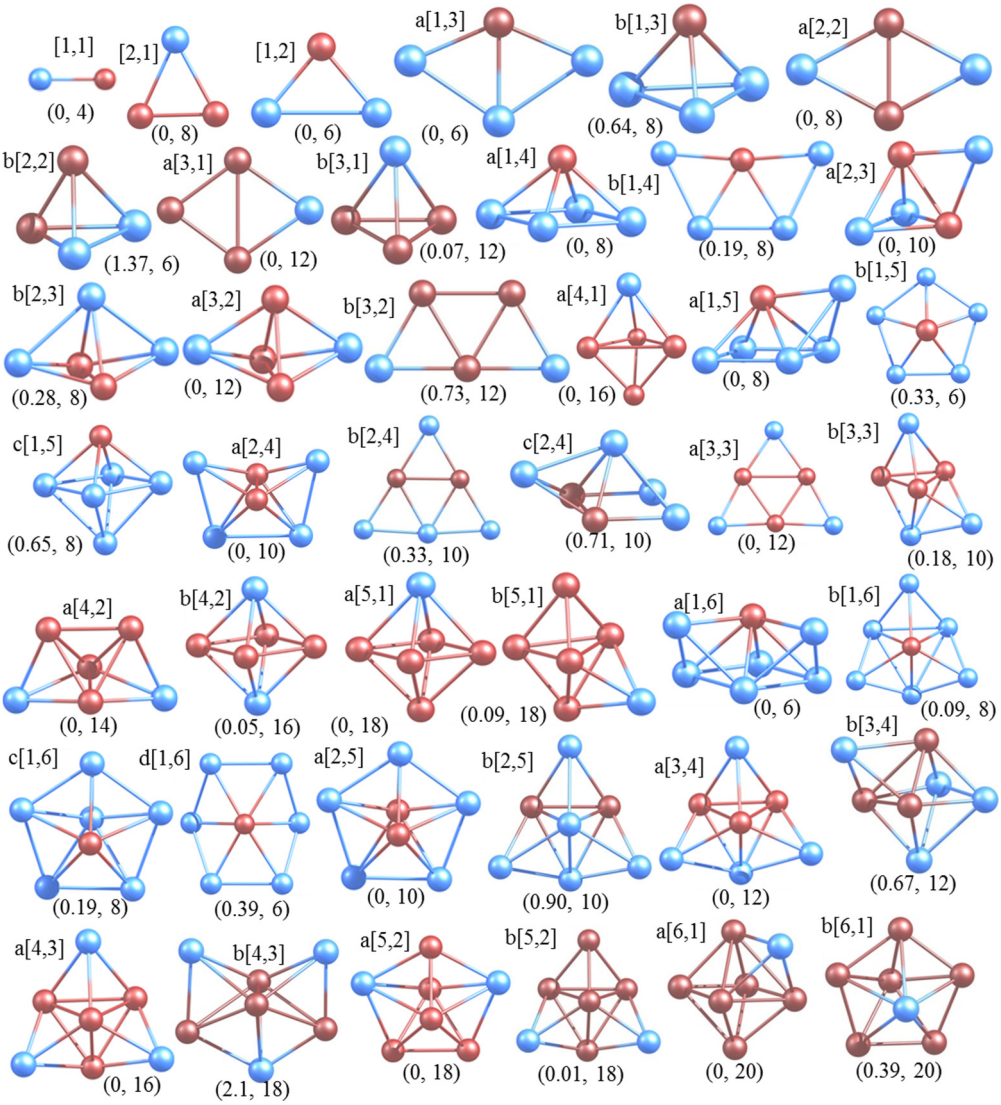

FIG. 2. (Color online) The low lying isomers of Fe-Pt clusters for $N = m + n = 2$–7. Here $z[m,n]$ refers to isomers $z = \text{a,b,}\ldots$ in increasing order of energy for a cluster with m (n) Fe (Pt) atoms. The numbers in brackets below the structures refer to the energy (eV) relative to the lowest energy isomer and the magnetic moment (μ_B). Red (blue) balls represent Fe (Pt) atoms.

B. Fe_mPt_n clusters with $m + n = 2$–5

The optimized low lying isomers of Fe_mPt_n clusters for $m + n = 2$ to 5 are shown in Fig. 2. There is strong bonding between Fe and Pt atoms as the BE for the FePt dimer is 2.18 eV/atom compared with the value of 1.60 and 1.95 eV/atom for Fe_2 and Pt_2, respectively. Pt_2 and Fe_2 dimers have 2 and 6 μ_B magnetic moments, respectively, whereas the FePt dimer has 4 μ_B magnetic moments. The bond length (2.18 Å) of the FePt dimer is nearly the mean of the bond lengths (2.33 and 2.01 Å, respectively) for Pt_2 and Fe_2. The Bader charge analysis gives about half an electron charge transfer from Fe to Pt atom with 3.4 and 0.59 μ_B magnetic moments on Fe and Pt, respectively. Fe_2Pt and $FePt_2$ clusters have triangular structures as for Pt_3 and Fe_3. There are 8 μ_B magnetic moments on Fe_2Pt with $\sim$3.53 μ_B on each Fe and 0.94 μ_B on Pt atom. This means that the addition of a Pt atom to Fe_2 results in an *increase* in the magnetic moments on Fe atoms. However, $FePt_2$ has 6 μ_B magnetic moments with 3.64 μ_B on Fe and 1.18 μ_B on each Pt atom. Accordingly, *the addition of a Fe atom to* Pt_2 *has increased the magnetic moments on Pt atoms, while there is a decrease in the magnetic moment of a Fe atom.*

The atomic structures of $FePt_3$, Fe_2Pt_2, and Fe_3Pt clusters are shown in Fig. 2. $FePt_3$ is similar to Pt_4 (Fig. 1). The Fe atom interacts with all the Pt atoms in a planar structure and the magnetic moment is 6 μ_B. Interestingly elemental Pt_3 has zero magnetic moment but the addition of a Fe atom leads to a high magnetic moment as the coupling becomes ferromagnetic. The magnetic moment on Fe atom is 3.64 μ_B while on Pt atoms, 0.95, 0.7, and 0.7 μ_B. Again the magnetic moment on a Fe atom is reduced by the interaction with Pt_3. A tetrahedron (isomer b[1,3]) in which Fe atom caps on three Pt atoms is 0.64 eV higher in energy with 8 μ_B magnetic moments. Fe_2Pt_2 is a capped Fe_2 dimer forming a rhombus with 8 μ_B magnetic moments. This is twice the value of the magnetic moments on a FePt dimer. Note that Fe_2Pt_2 can be considered as two FePt dimers interacting together. From Bader charge analysis the magnetic moments on each Fe (Pt) atom are 3.45 (0.55) μ_B.

Therefore the magnetic moment of Fe_2 increases when two Pt atoms interact with it. The Fe-Pt bond length increases to 2.37 Å. A tetrahedron (isomer b[2,2]) with 6 μ_B magnetic moments is 1.37 eV higher in energy. So a low dimensional structure is significantly more favorable. The lowest energy isomer of Fe_3Pt is the one in which a Pt atom caps on a side of Fe_3. It has 12 μ_B magnetic moments. As the magnetic moment on elemental Fe_3 is 10 μ_B, the addition of a Pt atom *increases* its magnetic moment by 2 μ_B. In this alloyed cluster the magnetic moments on Fe (Pt) atoms are quite large with the values of 3.81, 3.81, and 3.46 (0.91) μ_B. *The larger magnetic moments are on those Fe atoms that interact directly with Pt*. Interestingly in this case *the magnetic moments on Fe atoms are larger than in elemental* Fe_3. A tetrahedron (isomer b[3,1]) with Pt atom capped on three Fe atoms is only 0.07 eV higher in energy with the same total magnetic moments.

$FePt_4$ is a square pyramid with a Fe atom capping a Pt_4 square with 8 μ_B magnetic moments. Elemental Pt_4 as well as a Fe atom has 4 μ_B magnetic moments. After alloying the magnetic moment on the Fe atom is reduced to 3.61 μ_B but it is increased to ~1.09 μ_B on each Pt atom. The Fe-Pt (Pt-Pt) bond length is 2.39 Å (2.61 Å). Another isomer b[1,4] in which a Pt atom caps the lowest energy isomer of $FePt_3$ is only 0.19 eV higher in energy and again it has 8 μ_B magnetic moments. For Fe_2Pt_3, an isomer with a Pt atom capping the isomer b[2,2] of Fe_2Pt_2 on a side has the lowest energy with 10 μ_B magnetic moments. In this case the magnetic moments on each Fe atom are 3.54 μ_B which is higher compared to the value in Fe_2, while on Pt atoms the magnetic moments are 1.09, 1.09, and 0.72 μ_B which represent an *increase* compared with the value for Pt_3. Isomer b[2,3] in Fig. 2 is a Fe_2 dimer capped with three Pt atoms. It is 0.28 eV higher in energy and has 8 μ_B magnetic moments. A trigonal bipyramid with two Pt atoms capping a triangle of Fe_3 has the lowest energy for Fe_3Pt_2 with 12 μ_B magnetic moments. The Fe atoms have 3.67, 3.67, and 3.37 μ_B magnetic moments, while the value for each Pt atom is 0.65 μ_B. The magnetic moments on the three Fe atoms are *increased* compared with the value in the free Fe_3 cluster. The Fe-Pt bond lengths are 2.43, 2.47, and 2.47 Å, while Fe-Fe bond lengths are 2.41, 2.29, and 2.29 Å. The two Fe atoms with longer Fe-Pt bond lengths have higher magnetic moments. An isomer in which a Pt atom caps on a side of the lowest energy isomer of Fe_3Pt is 0.73 eV higher in energy with the same magnetic moments as in the lowest energy isomer. Note that Fe_3 (triangle) and Fe_3Pt (tetrahedral isomer) have 10 and 12 μ_B magnetic moments, respectively. So the addition of one more Pt atom in the latter isomer does not affect its total magnetic moments. For Fe_4Pt, a trigonal bipyramid (Pt atom capping a Fe_4 tetrahedron) is the lowest in energy with 16 μ_B magnetic moments. This is a large magnetic moment. The addition of a Fe (Pt) atom on Fe_3Pt (Fe_4) increases its magnetic moment by 4 (2) μ_B. The magnetic moments on each Fe atom interacting with the Pt atom are high (3.85 μ_B), while the Fe atom away from the Pt atom has 3.44 μ_B magnetic moments. This is close to the value (3.5 μ_B) in Fe_4 cluster. There is ~0.25 e charge transfer from each of the three Fe atoms to Pt atom and this contributes to the increase in the magnetic moments on these Fe atoms. The Pt atom has the magnetic moment of 1.02 μ_B. The Fe-Pt bond lengths increase to about 2.41 Å.

Our results on these small Fe-Pt clusters show that Fe atoms tend to occupy high coordination sites, while Pt atoms tend to occupy low coordination sites. In general, Fe-rich clusters have close packed structures, but Pt-rich clusters have relatively open structures. In all cases Fe atoms as well as in most cases Pt atoms have high magnetic moments. This is because in this size range pure Fe clusters themselves have large magnetic moments. These are further enhanced in some cases when alloyed with Pt and in some other cases there is a small decrease in the magnetic moments on a Fe atom. This is due to significant charge transfer (on an average ~0.65 e) on each Pt atom as well as hybridization between Fe and Pt states as we shall discuss later. The Bader charge analysis shows that the charge transfer is predominantly from those Fe atoms that interact with Pt atoms.

C. Fe_mPt_n clusters with $m + n = 6$ and 7

Some of the low lying isomers for $m + n = 6$ are shown in Fig. 2. The lowest energy isomer of $FePt_5$ has one Pt atom capping a square pyramid of $FePt_4$. The Fe atom interacts with all the Pt atoms and has 3.55 μ_B magnetic moments, while the Pt atoms have 1.00, 0.99, 0.89, 0.9, and 0.67 μ_B. Thus the planar structure of Pt_6 transforms to a 3D structure when one Pt atom is replaced by a Fe atom. Both $FePt_5$ and $FePt_4$ have 8 μ_B magnetic moments. Another isomer b[1,5] in which a Fe atom caps a Pt_5 pentagon lies 0.33 eV higher in energy and has 6 μ_B magnetic moments, while an isomer c[1,5] forming an octahedron lies 0.65 eV higher in energy with 8 μ_B magnetic moments. For Fe_2Pt_4 also a 3D structure (isomer a[2,4]) has the lowest energy. There are three interlinked tetrahedra around a Fe_2 dimer so that Fe-Pt bonds are optimal. From Bader charge analysis the magnetic moments on each Fe atom are 3.48 μ_B, while on Pt atoms the values are 0.81, 0.81, 0.71, and 0.71 μ_B. A planar triangular isomer b[2,4] with Fe_2 dimer interacting with all the Pt atoms is 0.33 eV higher in energy while another isomer c[2,4] lies 0.71 eV higher in energy. These isomers have the same magnetic moments of 10 μ_B. However, interestingly, for Fe_3Pt_3 an isomer a[3,3] derived from the Pt_6 triangular planar structure has the lowest energy with 12 μ_B magnetic moments. In this isomer Fe atoms occupy the central triangle as shown in Fig. 2. The magnetic moments on Fe atoms are 3.36, 3.41, and 3.40 μ_B, while on Pt atoms the values are 0.6, 0.6, and 0.64 μ_B. The total magnetic moments on Fe_3 seem to remain nearly the same as in elemental Fe_3 after alloying. The Fe-Pt bond lengths are shorter (~2.34 Å) because of the 2D structure. An isomer b[3,3] with a side-capped trigonal bipyramid is only 0.18 eV higher in energy with 10 μ_B magnetic moments. The lowest energy isomer of Fe_4Pt_2 is a bicapped Fe_4 tetrahedron and it is obtained by capping a Pt atom to isomer a[4,2] of Fe_4Pt. It has a total of 14 μ_B magnetic moments (the same as for Fe_4) with 3.35, 3.35, 3.14, and 3.14 μ_B on Fe atoms and 0.51 μ_B on each Pt atom. In this case the magnetic moments on Fe atoms are *decreased* compared with the value in pure Fe_4. The Fe-Pt bond lengths are 2.43 and 2.47 Å, while the Fe-Fe bond lengths are 2.30, 2.37, and 2.42 Å. From Bader charge analysis there is 0.67 e charge transfer to each Pt atom. An octahedral isomer b[4,2] with a bicapped Fe_4 square is only 0.05 eV higher in energy with 16 μ_B magnetic moments. In this case both Pt atoms interact with all the Fe atoms and the

magnetic moments are higher (3.51, 3.54, 3.54, and 3.54 μ_B on Fe atoms and ~0.93 μ_B on each Pt atom) compared with isomer a[4,2]. For Fe_5Pt the lowest energy isomer a[5,1] is a Fe_5 square pyramid capped with a Pt atom. It has 18 μ_B magnetic moments. The magnetic moments on Fe atoms are 3.49, 3.49, 3.49, 3.50, and 3.19 μ_B, while the Pt atom has 0.84 μ_B. The larger magnetic moments are on those Fe atoms that interact directly with Pt and transfer charge to it while the charge transfer from the remaining Fe atom is negligible. The total magnetic moments are the same as in pure Fe_5 and there is an effective decrease in the magnetic moments on Fe atoms by alloying with Pt. Another isomer b[5,1] with a Pt atom capping a side of a trigonal bipyramid has the same magnetic moments as in isomer a[5,1], and it lies only 0.09 eV higher in energy.

$FePt_6$ is a square pyramid of $FePt_4$ which is capped with Pt atoms on two faces (isomer a[1,6]). It has 6 μ_B magnetic moments. Note that *pristine* Pt_6 *cluster has zero magnetic moment due to ferromagnetic as well as antiferromagnetic coupling but the addition of one Fe atom makes the coupling in* $FePt_6$ *cluster ferromagnetic leading to high magnetic moments*. The Fe atom has 3.51 μ_B magnetic moments, while the Pt atoms have between 0.26 and 0.55 μ_B. One can also say that the planar structure of Pt_7 transforms to a three-dimensional (3D) structure by the replacement of one Pt atom with Fe. Another isomer b[1,6] with two Pt atoms capping a $FePt_4$ trigonal bipyramid lies only 0.09 eV higher in energy with 8 μ_B magnetic moments, while a pentagonal bipyramid (isomer c[1,6]) with 8 μ_B magnetic moments lies 0.19 eV higher in energy. On the other hand, a hexagonal isomer d[1,6] with a Fe atom at the center has 6 μ_B magnetic moments and lies 0.39 eV higher in energy. Therefore, *the addition of a Fe atom to* Pt_6 *converts a planar structure in to a 3D structure and leads to large magnetic moments*.

For Fe_2Pt_5, a pentagonal bipyramid (isomer a[2,5]) with the two Fe atoms at the apex sites and base as Pt_5 pentagon has the lowest energy. Each of the Fe atoms interacts with all the Pt atoms and has 3.39 μ_B magnetic moments, while the value for each Pt atom is 0.64 μ_B. There is a charge transfer of about 0.8 e from each Fe atom to Pt atoms and the excess charge on each Pt atom is about 0.3 e. In spite of the large charge transfer from Fe atoms, the magnetic moment is lower compared with the value in the free Fe atom. A trigonal bipyramid (isomer b[2,5]) in which a Pt atom caps isomer b[2,5] of Fe_2Pt_4 is 0.9 eV higher in energy. Both of these isomers have 10 μ_B magnetic moments. The addition of a Pt atom to isomer b[3,3] of Fe_3Pt_3 leads to the lowest energy isomer of Fe_3Pt_4. In this case each Fe atom has 3.33 μ_B magnetic moments, while the Pt atoms have 0.47, 0.48, 0.48, and 0.58 μ_B magnetic moments. The charge transfer from Fe atoms is 0.6, 0.7, and 0.58 e, while the excess charge on Pt atoms is 0.33, 0.47, 0.6, and 0.48 e. A Pt atom capped Fe_3Pt_3 octahedron (isomer b[3,4]) is 0.67 eV higher in energy with 12 μ_B magnetic moments.

The atomic structure of Fe_4Pt_3 is obtained by capping three Pt atoms on faces of a Fe_4 tetrahedron. It has 16 μ_B magnetic moments. The magnetic moments on Fe atoms are 3.48, 3.37, 3.46, and 3.46 μ_B, while on each Pt atom the value is ~0.74 μ_B. The charge transfer to each Pt atom is about 0.64 e. There is a slight decrease in the magnetic moments on Fe atoms compared with the value in the free Fe_4 cluster. An isomer b[4,3] in which two trigonal bipyramids fuse to form Fe_4Pt_3 with no two Pt atoms interacting directly lies 2.1 eV higher in energy with 18 μ_B magnetic moments. A trigonal bipyramid Fe_3Pt_2 capped with a Fe_2 dimer forming a pentagonal bipyramid has the lowest energy for Fe_5Pt_2 with 18 μ_B magnetic moments. Each Pt atom has 0.71 μ_B magnetic moments and about 0.62 e excess of charge. A Fe_5 trigonal bipyramid capped with two Pt atoms (isomer b[5,2]) is nearly degenerate (only 0.01 eV higher in energy) with the same magnetic moments. Note that *these nanoalloys have the same magnetic moments as elemental* Fe_5. *Since Pt atoms develop magnetic moments, there is a decrease in the magnetic moments on* Fe_5 *when Pt atoms are added. Thus charge transfer from Fe to Pt atoms does not necessarily increase their magnetic moments. Our results show that this is true in some cases such as in* Fe_4Pt *but not always.* Another isomer c[5,2] with a Fe_5 square pyramid and two Pt atoms capping on faces is 0.56 eV higher in energy with 18 μ_B magnetic moments. For Fe_6Pt a Fe_6 octahedron capped with a Pt atom (a[6,1] in Fig. 2) has the lowest energy with 20 μ_B magnetic moments. The magnetic moment on a Pt atom is 0.7 μ_B and the three Fe atoms interacting with it lose about 0.25 e each and have higher magnetic moments of 3.27 μ_B compared with the other three Fe atoms each of which has 3.16 μ_B. The charge on these three Fe atoms is close to the value in a pure Fe_6 cluster. These results suggest that there is a small decrease in the magnetic moments on Fe_6 when a Pt atom interacts with it. A pentagonal bipyramid with a Pt atom capping the Fe_5 pentagon base is 0.39 eV higher in energy with the same magnetic moments. These results show that with the increase in the cluster size the magnetic moments on Fe atoms tend to decrease. This aspect has been demonstrated in Fig. 3 where we have plotted magnetic moments on Fe atoms for all the clusters in the lowest energy configuration. The magnetic moments on

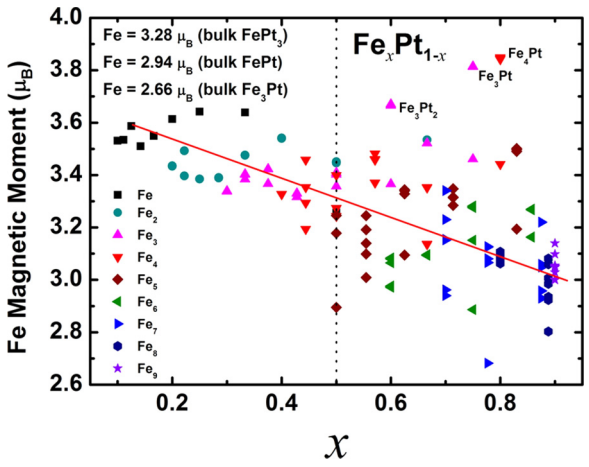

FIG. 3. (Color online) Magnetic moments on Fe atoms in Fe_mPt_n clusters. The points denoted by different symbols correspond to clusters with one, two, three, . . . , nine Fe atoms. x is the fraction of Fe atoms in the nanoalloy clusters. Also we have given the magnetic moments in three bulk phases for comparison. The magnetic moments have a decreasing tendency from a high value for small number of Fe atoms to lower values with increasing number of Fe atoms in Fe-Pt clusters. The line is drawn to aid the eyes. The magnetic moments are generally higher in clusters than in the corresponding bulk phase.

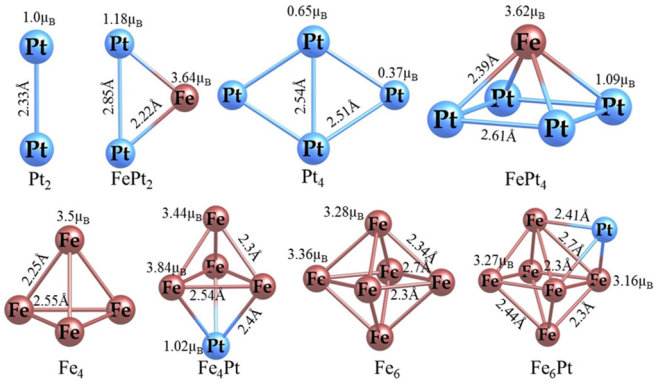

FIG. 4. (Color online) The bond lengths and magnetic moments on a few small Pt, Fe, and Fe-Pt clusters. One can note large magnetic moments on Fe atoms as well as increased magnetic moments on Pt atoms (compared with the values for elemental Pt clusters) in Pt-rich Fe-Pt clusters. For Fe-rich Fe_4Pt cluster, three Fe atoms connected with the Pt atom have higher magnetic moments compared with the case of Fe_4, whereas for Fe_6Pt the magnetic moments on Fe atoms connected with the Pt atoms are decreased.

Fe atoms are large for Pt-rich clusters generally and also for small Fe-rich clusters. As we shall see, this trend continues for $N = 8$–10 cases also. Overall there is a decreasing trend in the magnetic moments on Fe atoms as the cluster size and the number of Fe atoms increase. Figure 4 shows the bond lengths and local magnetic moments on Fe and Pt atoms in a few small pure Fe, pure Pt, and Fe-Pt clusters. One can notice large magnetic moments on Fe atoms as well as Pt atoms in Pt-rich clusters.

D. Fe_mPt_n clusters with $m + n = 8$

The optimized structures for $m + n = 8$ are shown in Fig. 5. The lowest energy isomer a[1,7] of $FePt_7$ has the same structure as Pt_8 (Fig. 1) with one of the capping atoms replaced with Fe. It has 6 μ_B magnetic moments with the Fe atom having 3.59 μ_B and the Pt atoms having 0.2 to 0.39 μ_B. The charge transfer from the Fe atom is ~0.9 e. A $FePt_4$ square pyramid capped with three Pt atoms (isomer b[1,7] in Fig. 5) is 0.07 eV higher in energy with the same magnetic moments. For Fe_2Pt_6 an isomer, a[2,6] with two inverted fused square pyramids sharing a Fe_2 dimer, has the lowest energy with 10 μ_B magnetic moments. In this case the magnetic moments on each Fe atom are 3.38 μ_B, while on each Pt atom, 0.54 μ_B. The charge transfer from each Fe atom is about 0.81 e, while the excess charge on Pt atoms lies in the range of 0.23 to 0.29 e. In this case the magnetic moments on Fe atoms are higher compared with the value for pure Fe_2. Another isomer with two fused square pyramids (b[2,6] in Fig. 5) and 8 μ_B magnetic moments lies 0.33 eV higher in energy. For Fe_3Pt_5 a tricapped trigonal bipyramid is the lowest in energy with 14 μ_B magnetic moments (a[3,5] in Fig. 5). The magnetic moments on Fe (Pt) atoms lie in the range of 3.37–3.42 (0.73–0.79) μ_B. Accordingly, the total magnetic moments on the three Fe atoms in the nanoalloy remain nearly the same as in pure Fe_3 cluster. An isomer with a bicapped octahedron (b[3,5] in Fig. 5) is 0.31 eV higher in energy with the same magnetic moments. On the other hand, a highly stable symmetric Fe_4 tetrahedron with all faces capped with Pt atoms is the lowest in energy for Fe_4Pt_4 (a[4,4] in Fig. 5) with 16 μ_B magnetic moments. The Fe (Pt) atoms have 3.24–3.39 (0.63–0.77) μ_B magnetic moments. There is charge transfer in the range of 0.55–0.72 e from Fe to Pt atoms, but the total magnetic moment on Fe_4 tetrahedron in the nanoalloy is slightly lower than the value in elemental Fe_4. An isomer (b[4,4]) with bicapped octahedron is 1.2 eV higher in energy with the same magnetic moments. But for Fe_5Pt_3 a bicapped octahedron with Fe atoms forming a square pyramid (a[5,3] in Fig. 5) has the lowest energy with 18 μ_B magnetic moments. The magnetic moments on Fe (Pt) atoms lie in the range of 3.09–3.34 (0.45–0.67) μ_B with the charge transfer of 0.36–0.47 e from Fe atoms. The total magnetic moments on Fe atoms decrease compared with the value for elemental Fe_5 as the total magnetic moments on Fe_5 and Fe_5Pt_3 are the same. An isomer with Pt capped pentagonal bipyramid (c[5,3]) is only 0.12 eV higher in energy. For Fe_6Pt_2 also a Fe_6 octahedron bicapped with Pt atoms is the lowest in energy with 20 μ_B magnetic moments. The Fe (Pt) atoms have 2.89–3.28 (0.42) μ_B magnetic moments. The charge transfer from Fe atoms decreases as the number of Pt atoms becomes less. Both Fe_6Pt_2 and Fe_6 have the same magnetic moments and therefore effectively the addition of Pt_2 to Fe_6 reduces its magnetic moments. An isomer with a pentagonal bipyramid capped with a Pt atom, b[6,2] is nearly degenerate with 0.07 eV higher energy. However, for Fe_7Pt a pentagonal bipyramid capped with a Pt atom, (a[7,1]) has the lowest energy with 22 μ_B magnetic moments, the same as for Fe_7. In this case the Fe (Pt) atoms have 2.93–3.22 (0.51) μ_B magnetic moments and the charge transfer is only from a few Fe atoms. An isomer with distorted Fe_2 capped octahedron lies 0.19 eV higher in energy. Again these results show that the magnetic moments on Fe atoms tend to decrease as the number of Fe atoms in the cluster increases and also generally when Pt atoms are added in small Fe clusters.

E. Fe_mPt_n clusters with $m + n = 9$

The optimized atomic structures of low lying isomers for $m + n = 9$ are shown in Fig. 5. $FePt_8$ is a tricapped octahedron (also view it as Pt_{10} with a vertex atom missing) with Fe atom at an apex site and interacting with six Pt atoms (a[1,8]). It has 10 μ_B magnetic moments. The magnetic moment on the Fe atom is 3.53 μ_B, while on Pt atoms it ranges from 0.58 to 1.04 μ_B. A pentagonal bipyramid bicapped with Pt atoms and Fe at the apex site (b[1,8]) lies 0.39 eV higher in energy with the same magnetic moments. Fe_2Pt_7 is a fused octahedron and a square pyramid with a common Fe_2 dimer, a[2,7]. It has 12 μ_B magnetic moments with 3.40 and 3.49 μ_B on Fe atoms and 0.6 to 0.83 μ_B on Pt atoms. There is 0.75 and 0.79 e charge transfer from Fe atoms. The magnetic moments on Fe_2 is increased in the nanoalloy due to interaction with Pt atoms. An isomer with two fused pentagonal bipyramids and Fe atoms at the nearest neighbor apex sites, b[2,7] is 0.22 eV higher in energy with the same magnetic moments. Fe_3Pt_6 is an octahedron with three Pt atoms capping the faces alternately in a symmetric fashion, a[3,6]. This can also be viewed as Pt_{10} tetrahedron with a vertex Pt atom missing and Fe_3 in the base. The magnetic moments on each Fe atom is about 3.4 μ_B, while on Pt atoms it lies in the range of 0.54 to 0.72 μ_B, the larger value being for Pt atoms

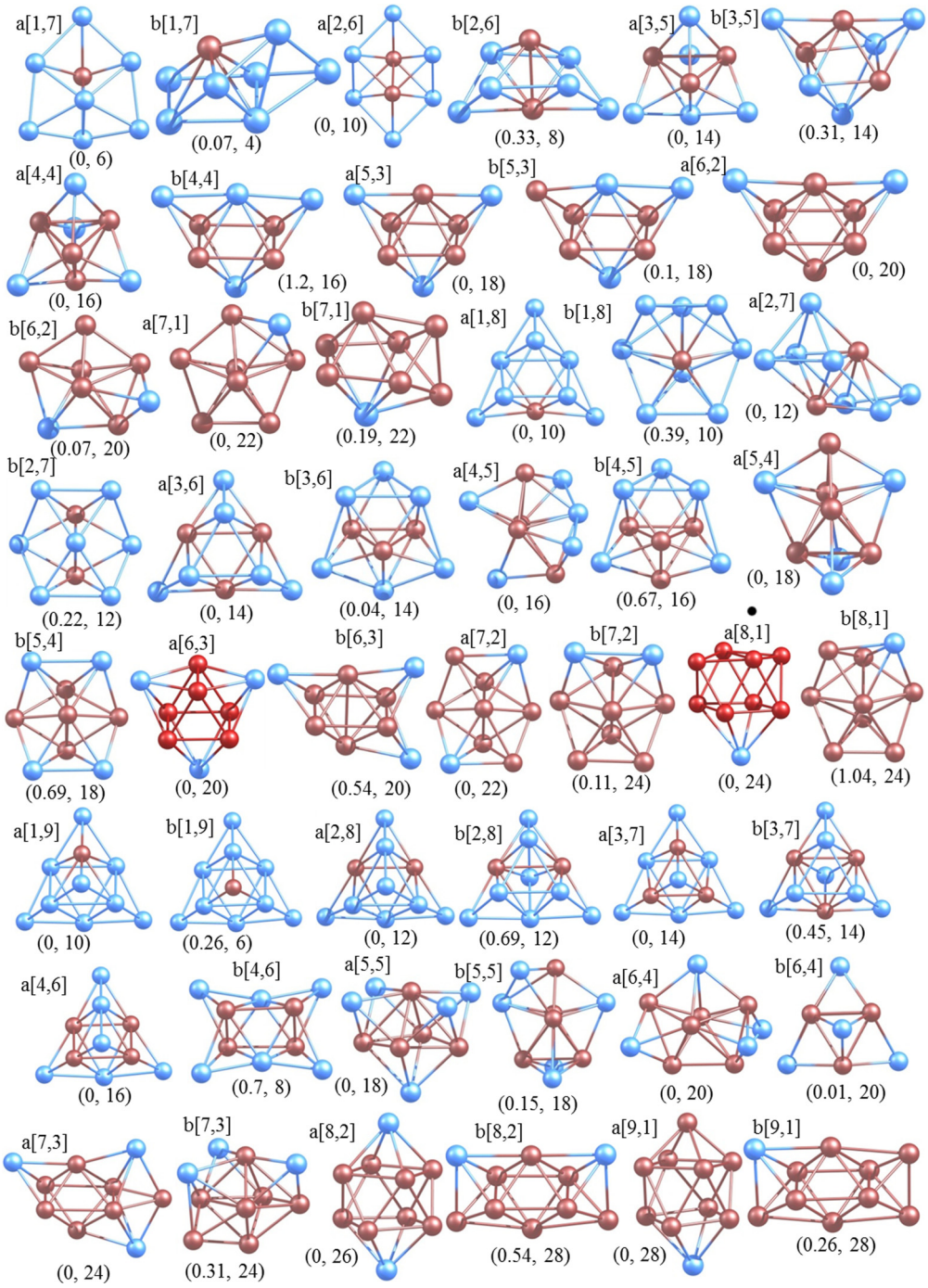

FIG. 5. (Color online) The same as in Fig. 2 but for $N = 8$–10.

interacting directly with Fe atoms. Another octahedral isomer in which three Pt atoms cap on three successive faces (b[3,6]) lies only 0.04 eV higher in energy. Both of these isomers have the same magnetic moment of 14 μ_B. Fe_4Pt_5 is a trigonal bipyramid with four Pt atoms capping on faces (a[4,5]). It has 16 μ_B magnetic moments with Fe (Pt) atoms having 3.19–3.46 (0.44–0.62) μ_B. There is charge transfer from Fe atoms in the range of 0.59 to 0.69 e. A tricapped octahedron containing a Fe_4 tetrahedron (b[4,5]) with the same magnetic moments is 0.67 eV higher in energy. However, Fe_5Pt_4 is a pentagonal bipyramid with two Pt atoms capping on opposite sides of an edge (a[5,4]). It has 18 μ_B magnetic moment which is the same as for pure Fe_5 and therefore effectively there is a decrease in the magnetic moments on Fe atoms due to alloying. As the size of the cluster as well as the number of Fe atoms increases, the magnetic moments on Fe atoms reduce as shown in Fig. 3. In this case the value for Fe (Pt) atoms lies in the range of 3.01–3.24 (0.51–0.63) μ_B. An isomer with four sides of a Fe_5 trigonal bipyramid capped with Pt atoms (b[5,4]) lies 0.69 eV higher in energy with the same magnetic moments. For Fe_6Pt_3, a Fe_6 octahedron tricapped with Pt atoms at alternate sites (a[6,3]) is the lowest in energy with 20 μ_B magnetic

moments. In this symmetric structure, each Fe (Pt) atom has 3.09 (0.48) μ_B magnetic moments. Note that a pentagonal bipyramid isomer (b[6,3]) lies only 0.07 eV higher in energy with 20 μ_B magnetic moments. These results show that often different low lying isomers for a given number of n and m have the same magnetic moments and also often the magnetic moments on the nanoalloy are the same as for the pure Fe cluster with the same number of Fe atoms as in the Fe-rich nanoalloy.

Fe_7Pt_2 has two interpenetrating pentagonal bipyramids with two Pt atoms lying farthest from each other (a[7,2]). It has 22 μ_B magnetic moments with Fe (Pt) atoms having 2.68–3.13 (0.38) μ_B. Another similar isomer in which a Pt dimer caps on a Fe_7 pentagonal bipyramid (b[7,2]) lies only 0.11 eV higher in energy with 24 μ_B magnetic moments. *These results suggest that the capped Pt atoms tend not to be near to each other as there is significant charge transfer.* Fe_8Pt is a Fe_7 pentagonal bipyramid capped with a FePt dimer (a[8,1]) as FePt dimer is energetically favorable. The magnetic moments on Fe atoms reduce further and lie in the range of 2.80–3.08 μ_B, while on the Pt atom, the value is 0.28 μ_B. An isomer with Fe_2 capping on a Fe_6Pt pentagonal bipyramid, b[8,1] lies 0.84 eV higher in energy with 24 μ_B magnetic moments.

F. Fe_mPt_n clusters with $m + n = 10$

The optimized structures of low lying isomers for $m + n = 10$ are shown in Fig. 5. $FePt_9$ is obtained from Pt_{10} (Fig. 1) by replacing the middle atom on an edge with Fe (a[1,9]). It has 10 μ_B magnetic moments with 3.53 (0.53–0.92) μ_B on Fe (Pt) atoms. There is 0.9 e charge transfer from Fe atom to four Pt atoms on which the magnetic moments are lower (0.53–0.55 μ_B), while the remaining five Pt atoms have 0.85–0.92 μ_B. In general, less charge transfer to Pt atoms leads to higher magnetic moments on them. An isomer (b[1,9]) in which an Fe atom replaces a vertex atom in Pt_{10} lies 0.26 eV higher in energy with 6 μ_B magnetic moments. This indicates that Fe atom prefers high coordination. Fe_2Pt_8, shown in a[2,8] has 12 μ_B magnetic moments. In this isomer when a top vertex Pt atom is moved to cap the Fe_2 side at the bottom in the same structure (b[2,8]), the energy becomes 0.69 eV higher and the magnetic moment is 12 μ_B. This result again supports the strong stability of the tetrahedral structure of Pt_{10} and its Pt-rich alloyed clusters. Making triangular Fe_3 in a[1,9] on a face of the octahedron (a[3,7]) leads to the lowest energy isomer for Fe_3Pt_7 with 14 μ_B magnetic moments. Note that an isomer in which Fe_3 is at the base and capped with a Pt atom (b[3,7]) lies 0.45 eV higher in energy with the same magnetic moments. Fe_4Pt_6 is a tetracapped octahedron with four Fe atoms at the base (a[4,6]) and 18 μ_B magnetic moments. A pentacapped square pyramid (a[5,5]) is the best structure for Fe_5Pt_5 with 18 μ_B magnetic moments, whereas with the same magnetic moments a pentagonal bipyramid with tricapping (b[5,5]) is 0.15 eV higher in energy. However, Fe_6Pt_4 is a pentagonal bipyramid with tricapping and 20 μ_B magnetic moments. A tetracapped trigonal prism (b[6,4]) lies only 0.01 eV higher in energy with 20 μ_B magnetic moments. Fe_7Pt_3 is a tricapped octahedron with Fe capping between Pt atoms (a[7,3]) and 24 μ_B magnetic moments. Another octahedral isomer, b[7,3], is 0.31 eV higher in energy. Fe_8Pt_2 is a tetragonal antiprism with two Pt atoms capped on opposite faces (a [8,2]) and 26 μ_B magnetic moments. A tetracapped (two Pt and two Fe atoms) Fe_6 octahedron as in b[8,2] lies 0.54 eV higher in energy with 28 μ_B magnetic moments. Fe_9Pt is also a bicapped tetragonal antiprism with one Pt at the apex site as in a[9,1] with 28 μ_B magnetic moments, while isomer b[9,1] is similar to b[8,2] but with only one Pt atom and it is 0.26 eV higher in energy. In these clusters as the number of Fe atoms increases, the magnetic moments on them decrease, e.g., from 3.43 μ_B for Fe_2Pt_8 to ~3 μ_B for Fe_9Pt. This trend is also seen in Fig. 3.

From our results of the atomic structures, we find that Fe atoms form the core in these clusters with higher coordination number, while Pt atoms tend to be on the surface at low coordination sites. There is charge transfer from Fe atoms to Pt atoms, in particular from those Fe atoms that are neighbors of Pt atoms. In general Pt-rich clusters have higher magnetic moments on Fe atoms, but small Fe-rich clusters also have large magnetic moments on Fe atoms. The magnetic moments on Fe atoms generally decrease with increasing cluster size. Also a larger charge transfer to Pt atoms leads to lower magnetic moments on them. Our results suggest that a charge transfer from Fe to Pt atoms does not always lead to an increase in the magnetic moments on Fe atoms compared to the value in the corresponding pure Fe cluster.

G. Binding energy, dipole moment, magnetic moments, and charge transfer

The BE calculated from PBE in VASP and HCTH/LANL2DZ in GAUSSIAN09 for the lowest energy isomers of clusters with different sizes and compositions is listed in Tables S2 and S3 of the Supplemental Material [39] and also shown in Fig. 6. As we discussed, the BE obtained by using PBE is overestimated and the one obtained by using HCTH/LANL2DZ in the GAUSSIAN09 program is closer to the experimental value where available, see Table S1 and Fig. S1 in the Supplemental Material [39]. However, the trends in the BE obtained from both methods are similar as there is a nearly rigid shift in the BE in PBE over HCTH/LANL2DZ value. Bulk Fe-Pt alloys have ordering tendency with the calculated cohesive energy of bulk FePt (Fe_3Pt) as 5.66 (5.43) eV/atom using PBE. Therefore, FePt alloy with equal concentration of Fe and Pt atoms is energetically most favorable. Our results show that the BE of Fe-Pt clusters also has the highest value near the equiatomic concentration, namely for $FePt_2$, Fe_2Pt_2, Fe_2Pt_3, Fe_2Pt_4, Fe_3Pt_4, Fe_4Pt_4, Fe_4Pt_5, and Fe_4Pt_6. The atomic structure also plays an important role as for some sizes and compositions, very symmetric structures are possible such as for Fe_4Pt_4. The BEs for Fe_2Pt_3 and Fe_3Pt_2 are almost equal with only 0.05 eV(0.11 eV) difference using PBE (HCTH/LANL2DZ). For $N = 6$, Fe_2Pt_4 and Fe_3Pt_3 are nearly degenerate with the difference of only 0.01 eV in both the methods. In the case of $N = 7$, Fe_2Pt_5 and Fe_3Pt_4 have a difference of only ~0.01 eV in the BE in both the methods. For $N = 9$, the difference in the BE of Fe_3Pt_6, Fe_4Pt_5, and Fe_5Pt_4 is about 0.03 eV which is similar in both the methods.

The dipole moments for the lowest energy isomers of the Fe_mPt_n ($m + n = 2$–10) clusters are obtained using HCTH/LANL2DZ in the GAUSSIAN09 program and are listed in Tables S2 and S3 in the Supplemental Material [39] and

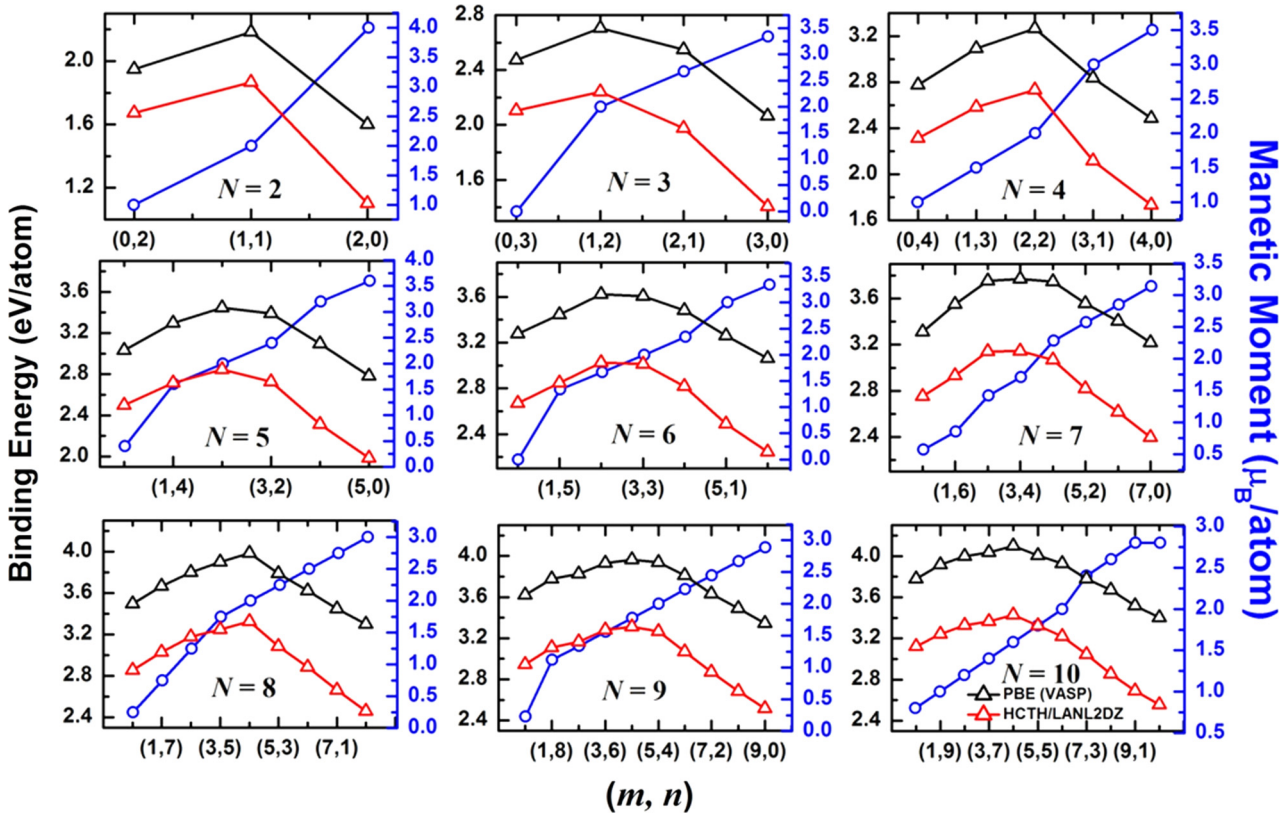

FIG. 6. (Color online) The binding energy (left y axis) and magnetic moments (right y axis) per atom as a function of the number of Fe and Pt (m, n) atoms in Fe_mPt_n clusters for different values of N. The magnetic moments are obtained by using PBE in VASP while the values of the binding energy are given by using PBE in VASP and HCTH in the GAUSSIAN09 program, both of which show similar trend as (m,n) are varied, but the values in the case of HCTH calculations are lower.

plotted in Fig. 7. The lowest energy isomers of Fe_2Pt_2, Fe_2Pt_5, Fe_2Pt_6, Fe_6Pt_3, and Fe_4Pt_6 have zero dipole moment and it is due to the symmetric structures of these clusters. Interestingly, the addition of a Fe (Pt) atom to a pure Pt (Fe) cluster shoots up the dipole moment to its maximum value and this value is higher than those associated with the pure clusters. This is due to the fact that there is quite significant charge transfer in these clusters (higher than expected in monoatomic clusters) as well as the absence of centrosymmetry [41,42]. For $N = 2$ and 3 the dipole moments are nonzero because there is no center of inversion symmetry, while for $N = 4$ the symmetric structure of the lowest energy isomer of Fe_2Pt_2 with equal composition leads to zero dipole moment. However, for the unequal compositions, i.e., Fe_3Pt and $FePt_3$, the structures are asymmetric and have large dipole moments. In the case of $N = 5$ and 6, almost zero dipole moments are obtained in the case of Fe_2Pt_5 and Fe_3Pt_3, respectively. On the other hand, for $N = 7$, Fe_2Pt_5 is highly symmetric and has zero dipole moment. For $N = 8$ zero dipole moment is associated with Fe_2Pt_6 and Fe_4Pt_4 clusters, while for $N = 9$ we find that Fe_6Pt_3 has zero dipole moment. For $N = 10$, Pt_{10} has zero dipole moment due to its symmetric tetrahedral structure, but when one Pt atom is replaced with an Fe atom, the symmetry is broken. Also it develops a slight change in the atomic structure due to the contraction in the bond lengths (i.e., the bond length of Pt-Pt is larger than the bond length of Fe-Pt). But for Fe_4Pt_6 the dipole moment suddenly becomes zero as there is a symmetric structure. A similar behavior can be seen in the case of Fe_8Pt_2.

We conclude here that in general clusters (except for FePt) with nearly equiatomic compositions have high BE and almost zero dipole moments due to symmetric (or near symmetric) structures. Large dipole moments (2–3 Debye) are observed for some Fe-rich as well as Pt-rich Fe-Pt clusters. The permanent electric dipole moments in these clusters suggest their ferroelectric behavior. In addition, these clusters are ferromagnetic. The coexistence of ferromagnetism and ferroelectric behavior in these clusters could lead to coupling between the two order parameters and a multiferroic behavior.

The local magnetic moments (see Fig. 3) and charge on each atom using Bader analysis (Fig. 8) are obtained by using PBE method in VASP. The total magnetic moments as obtained by using PBE in VASP and HCTH/LANL2DZ in the GAUSSIAN09 program are the same for the lowest energy structures. The total magnetic moments for the lowest energy isomers, charge, and local magnetic moments on Fe and Pt atoms in each isomer, and the number of first nearest neighbor (γ) for each atom of Fe_mPt_n ($m + n = 2$–10) clusters are given in Tables S5–S9 in the Supplemental Material [39]. In Fig. 3 the magnetic moments on each Fe atom in a cluster are plotted as a function of the concentration of Fe atoms in order to obtain the overall trend as a function of the cluster size. The magnetic moments on Fe atoms in Pt-rich clusters are large ($\sim$3.8 μ_B) and the value decreases to about 3 μ_B in Fe-rich clusters as the size

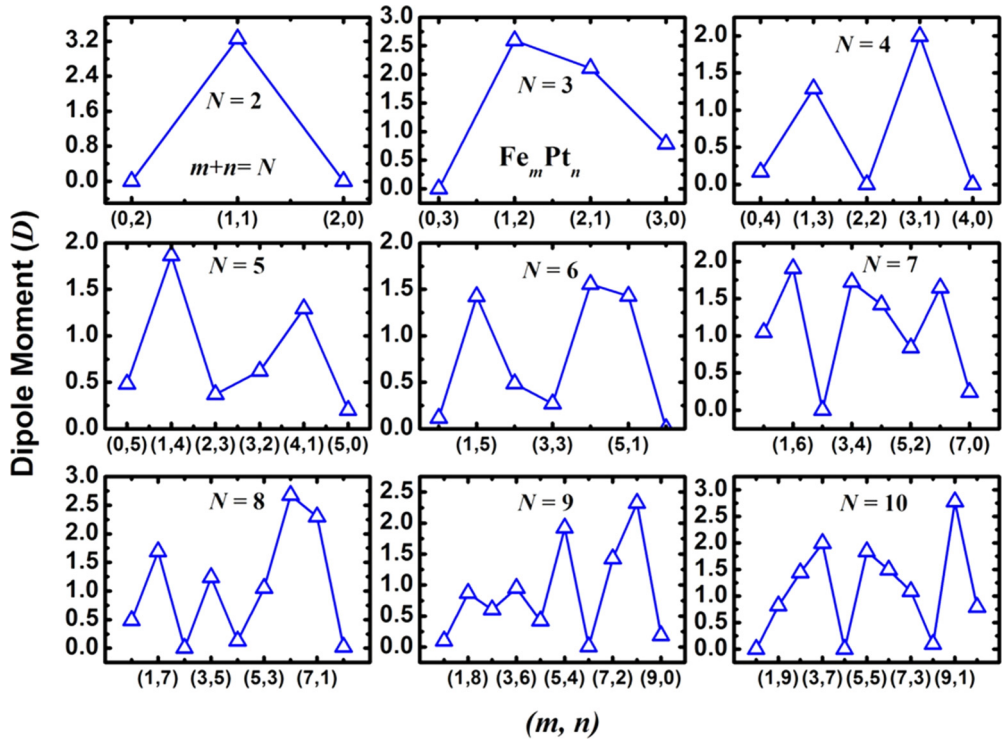

FIG. 7. (Color online) The electric dipole moment of Fe_mPt_n ($m + n = 2$–10) clusters using HCTH/LANL2DZ in the GAUSSIAN09 program as a function of the number of Fe and Pt atoms, i.e., (m, n) in Fe-Pt clusters for different values of $m + n = N$. The values close to zero are for (nearly) symmetric clusters.

increases. The magnetic moment on Pt atoms is about 1.0 μ_B in Pt-rich clusters and it is about 0.2 μ_B in the case of Fe-rich clusters. All the clusters have ferromagnetic coupling. The total magnetic moments per atom on a cluster are significantly higher than the value in the corresponding bulk and the value decreases as the cluster size as well as the number of Fe atoms in a given cluster increases. Figure S2 in the Supplemental Material [39] shows the magnetic moments on Fe atoms for different cluster sizes separately as a function of the number of Fe atoms in a cluster. It can be seen that the magnetic moments on Fe atoms in nanoalloy clusters are higher on some atoms and lower on a few other Fe atoms compared with the value for the pure Fe cluster of the same size as the nanoalloy cluster. In bulk Fe-Pt alloys the magnetic moments on Fe atoms are higher than in bulk Fe. The local magnetic moments of pure Fe clusters decrease with an increase in the coordination number of each atom, whereas in the case of Fe-Pt clusters it not only depends on the coordination number but also on the neighboring atoms.

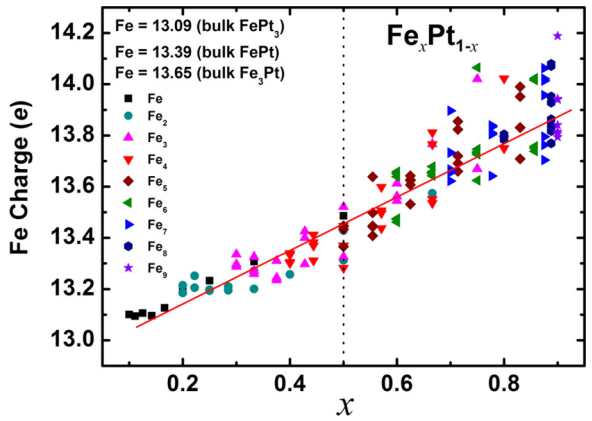

FIG. 8. (Color online) Bader electronic charge on Fe atoms in different clusters as a function of the Fe concentration (x) in Fe_mPt_n clusters. There is a decrease in the charge transfer from Fe atoms to Pt atoms as the number of Fe atoms increases in a cluster. A line is drawn to aid the eyes. Different symbols are for different numbers of Fe atoms in clusters. Note that the Fe atom has been considered to have 14 valence electrons and a value lower than 14 means charge transfer from Fe.

In general the charge on Fe atoms is depleted by about 0.7 e (Fig. 8) and the charge on Pt atoms is in excess by about 0.5 e, indicating charge transfer from Fe to Pt atoms. The charge transfer from Fe to Pt atoms is similar to the behavior in bulk Fe-Pt alloys and it depends on the composition, but it is less sensitive to the size of the clusters. A higher charge transfer to Pt atoms such as in Fe-rich clusters leads to lower magnetic moments on Pt atoms. In Fig. S3 (see Supplemental Material [39]) we have shown excess and depletion of charge for the lowest energy isomers of Fe_2Pt, Fe_3Pt, Fe_6Pt, Fe_4Pt_4, and Fe_4Pt_6. This has been obtained by subtracting the sum of the self-consistent charge of Fe atoms alone and Pt atoms alone at the same positions as in the alloy cluster from the total charge of the alloy cluster. The excess charge is seen around the Pt atoms, while the depletion of charge is seen around Fe atoms. Some rearrangement of charge also occurs around both Fe and Pt atoms. Also, both the charge transfer and magnetic moments have significant deviation from the values in the corresponding Fe clusters mostly for Fe and Pt atoms that interact together. Therefore, the charge transfer effect seems to be very local.

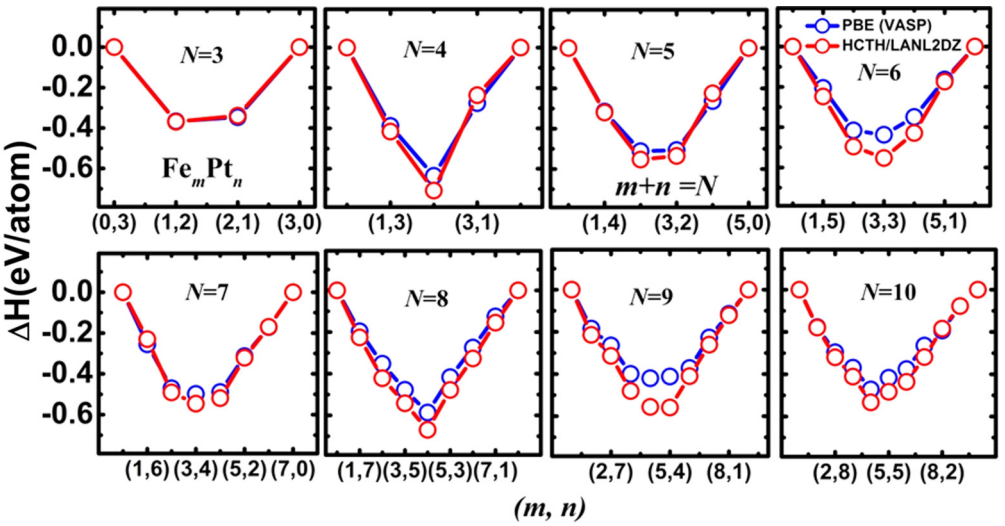

FIG. 9. (Color online) The heat of formation for Fe_mPt_n (m,n) clusters with $N = m + n$ calculated using PBE in VASP and HCTH/LANL2DZ in the GAUSSIAN09 program. Both methods give nearly the same behavior. A large negative value is obtained for approximately equiatomic concentration.

H. Heat of formation and second order difference of total energy

We have calculated ΔH and Δ_2 to find the relative stability of Fe-Pt clusters of different sizes and different compositions. If $E(A_mB_n)$ is the energy of a A_mB_n cluster of size $N = m + n$, then ΔH is defined as

$$\Delta H(A_mB_n) = E(A_mB_n) - m\frac{E(A_N)}{N} - n\frac{E(B_N)}{N}, \qquad (1)$$

i.e., subtracting from the energy of A_mB_n cluster the appropriate fraction of the energy of pure clusters (A_N and B_N) of the same size, while Δ_2 is defined as

$$\Delta_2(A_mB_n) = E(A_{m+1}B_{n-1}) + E(A_{m-1}B_{n+1}) - 2E(A_mB_n). \qquad (2)$$

Accordingly, clusters with large positive value of Δ_2 are highly stable. The calculated ΔH and Δ_2 of Fe_mPt_n clusters for $N = 2$–10 (the values are listed in Tables S2 and S3 in the Supplemental Material [39]) from PBE in VASP and HCTH/LANL2DZ in GAUSSIAN09 are shown in Figs. 9 and 10, respectively. It is interesting to note that the calculated ΔH values are consistent irrespective of the method used. It suggests that Fe-Pt clusters with nearly equiatomic concentration of Fe and Pt are more stable than clusters with compositions close to Fe_3Pt or $FePt_3$. This is similar to bulk behavior but in clusters as the atomic structure also plays an important role, we find that for $N = 10$ the largest ΔH is associated with Fe_4Pt_6 and not with Fe_5Pt_5 or Fe_6Pt_4. Fe_4Pt_6 has a tetrahedral structure based on Pt_{10} which is also a highly stable cluster, whereas Fe_5Pt_5 and Fe_6Pt_4 do not have high

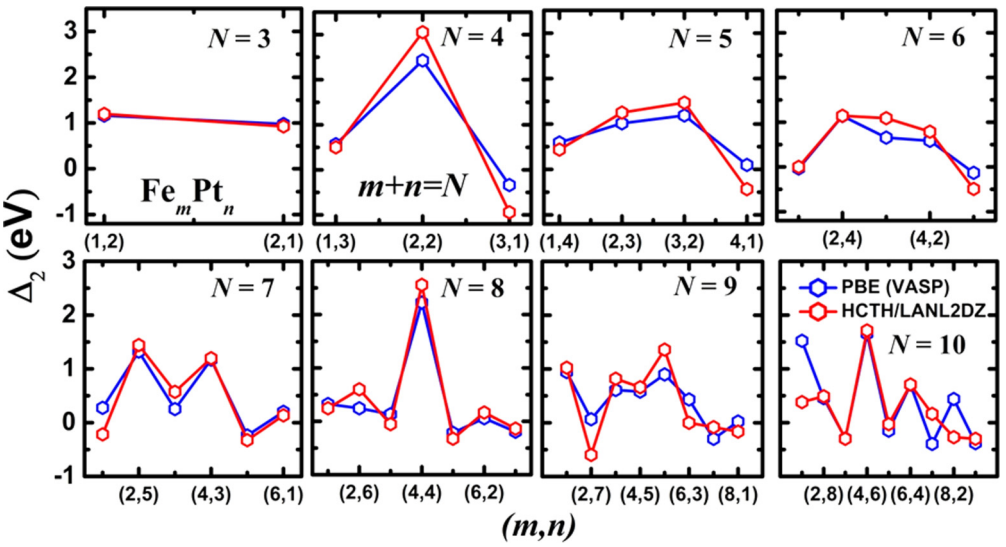

FIG. 10. (Color online) Second order difference of the total energy for different Fe_mPt_n clusters as a function of the number of Fe and Pt (m,n) atoms obtained by using PBE in VASP and HCTH/LANL2DZ in the GAUSSIAN09 program. Both methods give very similar behaviors. A positive value means that the particular cluster is strongly favorable.

symmetry structures. For $N = 9$ the largest ΔH is associated with Fe_4Pt_5 and Fe_5Pt_4 has a slightly less negative value. On the other hand for $N = 8$, Fe_4Pt_4 is highly stable with large heat of formation and it has a highly symmetric structure based on a tetrahedron. For $N = 7$, Fe_3Pt_4 has the largest ΔH value, while for Fe_4Pt_3 the value is less negative. For $N = 6$ Fe_3Pt_3 has the highest ΔH. For $N = 5$ Fe_2Pt_3 has the largest ΔH and for $N = 4$ it is Fe_2Pt_2. These results suggest that either $m = n$ has the largest ΔH or a slightly Pt-rich configuration has the largest value. Further clusters with $N = 4$ and 8 have the largest ΔH (about -0.7 eV per atom) with $m = n$ compared with other sizes. The Δ_2 values indicate relatively high stability for Fe_2Pt_2, Fe_3Pt_2, Fe_2Pt_4, Fe_2Pt_5, Fe_4Pt_4, Fe_5Pt_4, and Fe_4Pt_6 clusters using both PBE in VASP and HCTH/LANL2DZ in the GAUSSIAN09 program. Overall from the BE, ΔH, and Δ_2 calculations Fe_2Pt_2, Fe_4Pt_4, and Fe_4Pt_6 clusters stand out and are found to be the best from the stability point of view. Accordingly in experiments high abundance of these clusters is expected among Fe-Pt clusters.

I. Density of states

We discuss here the results of the electronic states for a few selected clusters. The spin-polarized densities of states (DOSs) for the lowest energy isomers of Fe_2Pt_2 and Fe_4Pt_4 clusters along with that of a FePt dimer obtained from PBE exchange-correlation functional are presented in Fig. S4 of the Supplemental Material [39]. Also we have shown the partial DOSs for Fe and Pt atoms. The DOSs of Fe-Pt clusters are dominated by d states of Fe and Pt atoms. The up spin d states of Fe atoms are generally fully occupied, while the down spin states are only partially occupied and this leads to large magnetic moments on Fe atoms. The up spin states of Pt atoms are also almost fully occupied and some down spin states lie above the highest occupied molecular orbital (HOMO) leading to relatively small magnetic moments on Pt atoms. As Pt atoms generally occupy low coordination sites in the clusters we have studied, there is in general a narrow distribution of their electronic states in spite of the fact that these are $5d$ states for Pt while $3d$ for Fe atoms. The $5d$ states of Pt atoms mostly lie between -8 and -5 eV, whereas the up spin $3d$ states of Fe atoms lie from -9 to -6 eV. As one can see from the partial DOSs of Fe and Pt atoms for Fe_4Pt_6 cluster (see Fig. S5 in the Supplemental Material [39]), Pt(1) atom has three nearest neighbors and narrow distribution of $5d$ states, but Pt(3) has six nearest neighbors (three Pt and three Fe) and the $5d$ states have a broader distribution. In Figs. 11 and 12 we have shown the total and partial DOSs for the lowest energy isomers of Fe_4Pt and Fe_6Pt clusters, respectively, along with the angular momentum resolved contributions from Fe ($3d$) and Pt ($5d$) to the electronic states of the cluster. These results show that in general there is significant hybridization between Fe and Pt d states. For these two clusters one can consider the atomic structure to arise from the interaction of a Pt atom on Fe_4 tetrahedral and Fe_6 octahedral clusters that are the lowest energy structures for elemental Fe_4 and Fe_6 clusters. Accordingly, we have also shown the DOS of elemental Fe_4 and Fe_6 clusters for comparison. It can be noted that the lowest unoccupied molecular orbital (LUMO) in the DOS has strong contribution from the down spin $3d$ states of

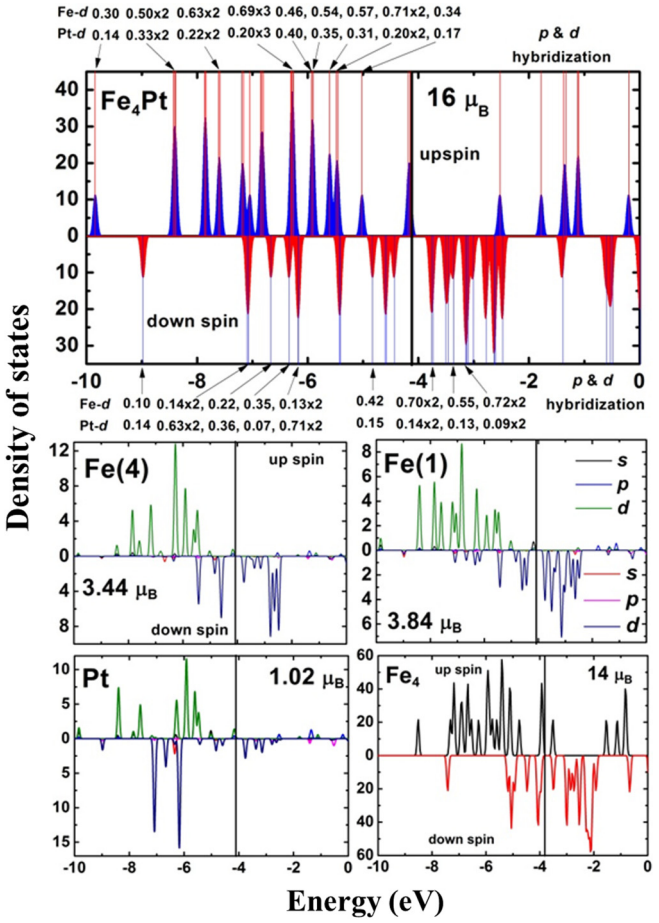

FIG. 11. (Color online) The total electronic up spin and down spin densities of states (number of states/cluster) of Fe_4Pt cluster are shown in the top panel. The numbers above and below this figure show the contributions of the $3d$ of Fe atoms and $5d$ of Pt atom to different states signifying strong hybridization. The states with $p - d$ hybridization are also seen above the LUMO. The up spin and down spin partial angular momentum resolved densities of states of Pt as well as inequivalent Fe atoms [Fe(1) and Fe(4)] are shown in the lower panels. Also, the total density of states for elemental Fe_4 cluster is shown. Vertical line shows the HOMO. The magnetic moments are also given for the whole cluster as well as for different atoms.

Fe atoms. Also the HOMO is primarily from Fe atoms with relatively small contribution from hybridization with Pt $5d$ states. Generally Pt $5d$ states lie slightly below the HOMO, whereas the states above the LUMO have strong $3d$ character of Fe and following these there are states with significant $p - d$ hybridization. The hybridization between the Fe and Pt states makes significant difference in the DOS of Fe_4 and Fe_4Pt as well as Fe_6Pt and Fe_6 clusters. An important aspect to note is that there is significant enhancement ($3.84\,\mu_B$) in the magnetic moments on Fe atoms that interact directly with a Pt atom as shown for the Fe_4Pt case in Fig. 11. This is compared to the value of $3.5\,\mu_B$/atom for elemental Fe_4. On the other hand, for Fe_6Pt the magnetic moments of Fe atoms that directly interact with Pt atoms decrease compared with the value for an elemental Fe_6 cluster even though in both clusters Fe_4Pt and Fe_6Pt there is significant charge transfer

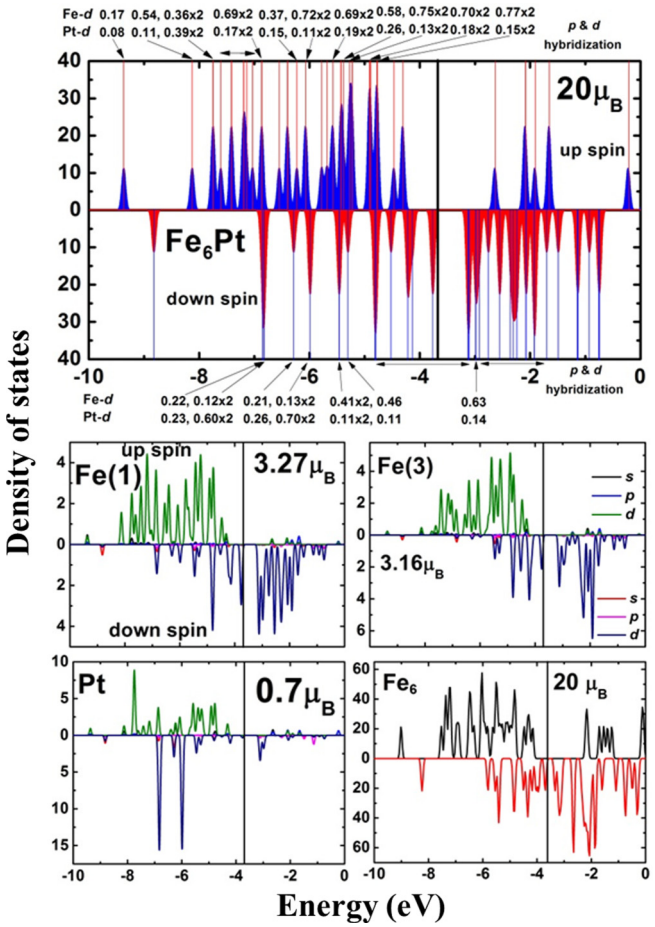

FIG. 12. (Color online) Top panel shows the total up spin and down spin electronic densities of states (number of states/cluster) of the Fe_6Pt cluster. The numbers below and above the figure show contributions of the *d* electrons of Fe and Pt atoms to different states. The partial densities of states of Pt as well as inequivalent Fe atoms [Fe(1) and Fe(3)] are shown in the lower panels. Also, the total density of states for elemental Fe_6 cluster is shown. The magnetic moments in different cases are given. The vertical line shows the HOMO.

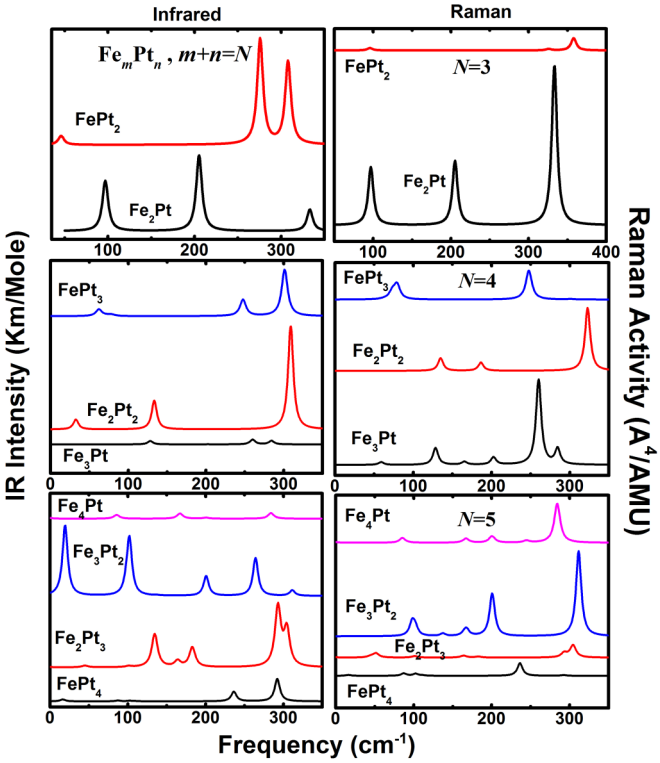

FIG. 13. (Color online) Infrared spectra (left) and Raman spectra (right) of Fe_mPt_n ($m+n=N=3$–5) clusters obtained by using HCTH/LANL2DZ in the GAUSSIAN09 program. The values of the intensities are given in Supplemental Material [39].

from Fe to Pt atoms. It has been considered that charge transfer from Fe atoms to Pt atoms could increase imbalance in the up and down spin contributions leading to enhancement in the magnetic moments on Fe atoms. However, our results suggest that it is more subtle and that the hybridization between the Fe and Pt states as well as the atomic structure also play an important role.

J. Infrared and Raman spectra

We have calculated IR and Raman frequencies for the lowest energy structures of Fe_N, Pt_N, and Fe_mPt_n ($m+n=N=2$–10) clusters. The calculated harmonic frequencies for all the structural isomers are found to be positive, which suggests the dynamical stability of these clusters. The harmonic frequency for FePt dimer is 314.12 cm^{-1}, which is associated with Fe-Pt stretching mode and it is IR and Raman active. In contrast, the harmonic frequencies for Fe_2 and Pt_2 dimers are only Raman active at 390.71 and 222.78 cm^{-1}, respectively. The IR and Raman spectra for all the lowest energy structures of Fe-Pt clusters are plotted in Figs. 13–15 (for pure Fe and Pt clusters it is given in the Supplemental Material [39] in Fig. S6). The frequencies and corresponding IR intensities and Raman activities of Fe-Pt clusters along with those of the pure Fe and Pt clusters are listed in Tables S10–S14 in the Supplemental Material [39]. For $N=3$ (i.e., $FePt_2$ and Fe_2Pt), the lowest harmonic frequencies are associated with Pt-Pt stretching (45.95 cm^{-1}) and Fe-Pt antisymmetric stretching (96.92 cm^{-1}) modes, respectively. The other two modes in $FePt_2$ at 275.82 and 308.04 cm^{-1} are Fe-Pt antisymmetric stretching and scissor modes, respectively (see Fig. 13). In the case of Fe_2Pt, the Fe-Pt and Fe-Fe stretching modes are at 205.27 and 333.23 cm^{-1}, respectively. All three modes of Fe_2Pt have higher Raman activity compared to the modes of $FePt_2$. For $N=4$, $FePt_3$, Fe_2Pt_2, and Fe_3Pt have similar structures. The higher intensity IR modes in $FePt_3$ and Fe_2Pt_2 are associated with 292.1 cm^{-1} (rocking mode) and 309.1 cm^{-1} (breathing mode), respectively. Fe_3Pt has less prominent IR modes compared with $FePt_3$ and Fe_2Pt_2. It has Raman activity at 260.2 cm^{-1} which corresponds to Fe-Pt stretching mode. For $N=5$, Fe_2Pt_3 and Fe_3Pt_2 have high intensity IR modes compared to Fe_4Pt and $FePt_4$. The IR modes (19.2 and 101.9 cm^{-1}) for Fe_3Pt_2 are basically the antisymmetric stretching modes of Fe-Fe bonds. There is high Raman activity in the case of Fe_3Pt_2 for Fe-Fe stretching mode at 311.5 cm^{-1}. In contrast, Fe_2Pt_3 has high intensity IR modes associated with stretching (300.1 cm^{-1}) and scissor (310.1 cm^{-1}) modes of Fe-Pt bonds. In Fig. 14 we have plotted IR and Raman spectra for $N=6$–8 of Fe_mPt_n clusters. For

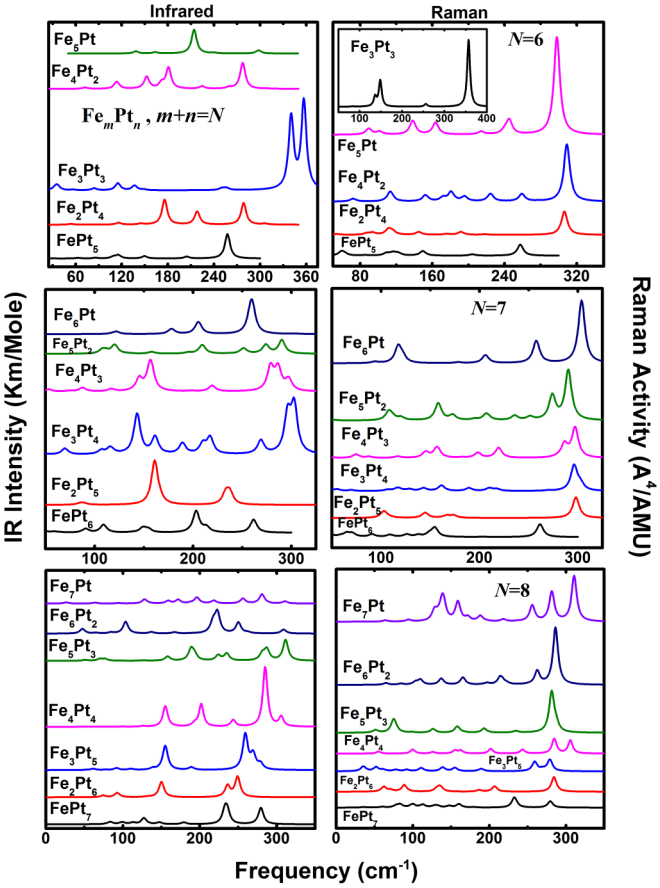

FIG. 14. (Color online) Infrared spectra (left side panel) and Raman spectra (right side panel) of Fe_mPt_n ($m+n=N=6$–8) clusters obtained by using HCTH/LANL2DZ in the GAUSSIAN09 program. The Raman spectrum for Fe_3Pt_3 is shown in the inset. The values of the intensities are given in Supplemental Material [39].

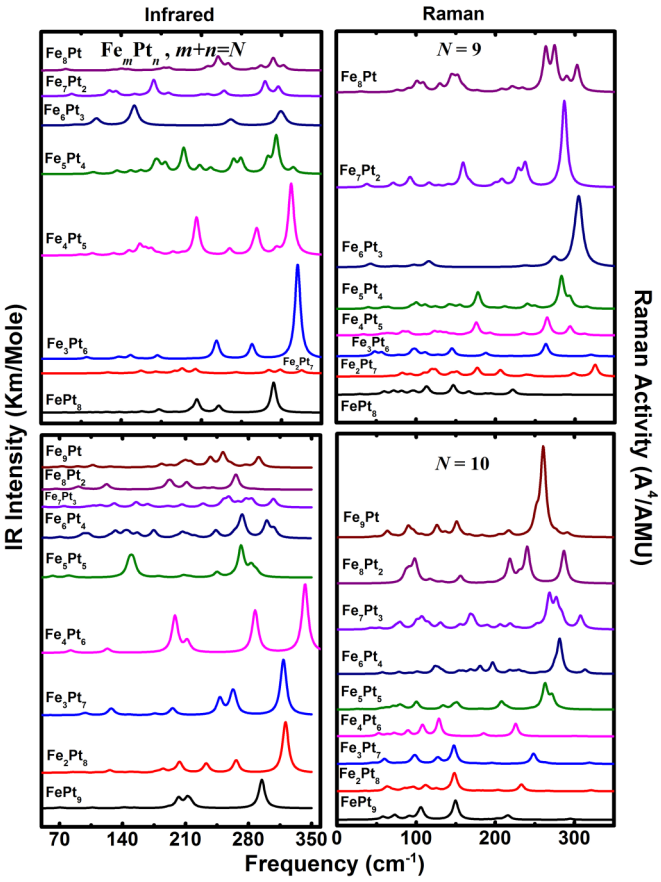

FIG. 15. (Color online) Infrared spectra (left side panel) and Raman spectra (right side panel) of Fe_mPt_n ($m+n=N=9$ and 10) clusters calculated by using HCTH/LANL2DZ in the GAUSSIAN09 program. The values of the intensities are given in Supplemental Material [39].

$N=6$, Fe_3Pt_3 has the highest IR intensity and Raman activity over other clusters. The symmetric stretching mode of Fe-Pt bond is at 356.9 cm^{-1}. This mode is found to be only Raman active. A symmetric breathing mode is obtained at 148.7 cm^{-1}. For $N=7$, Fe_4Pt_3, Fe_3Pt_4, and Fe_2Pt_5 clusters have almost equal intensity IR modes. The frequencies around 296 and 143 cm^{-1} are scissor and rocking modes of Fe-Pt bonds. The scissor mode around 296 cm^{-1} is absent in Fe_2Pt_5. Whereas this scissors mode of Fe-Pt bond is found to be Raman active in all the clusters. For $N=8$, Fe_4Pt_4 has the highest intensity IR mode over other compositions. This is associated with scissor mode of Fe-Pt bonds at 274 cm^{-1} and it is also Raman active. For $N=9$–10 (see Fig. 15), the Pt-rich clusters have the highest IR intensities, whereas the Fe-rich clusters have higher Raman activity. The highest intensity IR mode is at around 320 cm^{-1}, which is from Fe-Pt stretching, whereas the breathing mode is found to have higher Raman activity.

For a given size, the higher intensity IR modes are associated with the equiatomic compositions compared to the rest of the clusters. The Fe-Pt stretching modes are associated with the high frequency IR modes. The best structures of Fe-Pt clusters i.e., Fe_2Pt_2, Fe_3Pt_3, Fe_4Pt_4, and Fe_4Pt_6, exhibit the highest intensity IR modes due to more Fe-Pt bonds than in other compositions for a given size.

IV. SUMMARY

In summary, we have studied the evolution of the atomic structure and magnetic properties of Fe-Pt clusters having up to ten atoms. The lowest energy atomic structures of Fe-Pt clusters up to four atoms are planar, while larger clusters have 3D structures. This is in contrast to pure Pt clusters that have planar structures for larger sizes as well such as for Pt_6 and Pt_9. The most favorable distribution of Fe and Pt atoms is the one in which Fe atoms form the core with high coordination while Pt atoms occupy low coordination sites. Thus Fe atoms tend to aggregate together as core and Pt atoms segregate on the surface and cap this core. We believe that such a trend will continue for larger clusters of Fe-Pt before ordering will set in the whole cluster as it has been recently shown [43] for Fe-Pt nanoparticles. As in bulk, clusters with nearly equal number of Fe and Pt atoms have the largest BE as well as the largest formation energy. Among the different sizes and configurations, Fe_2Pt_2, Fe_4Pt_4, and Fe_4Pt_6 are the best from the point of view of BE, ΔH, and Δ_2. These clusters should be

abundant in experiments. The magnetic moments on Fe and Pt atoms are enhanced in Fe-Pt clusters with ferromagnetic coupling compared with the values in bulk Fe, bulk Pt, as well as in bulk Fe-Pt. The magnetic moments on Fe atoms reach a maximum value of 3.8 μ_B and on Pt atoms, a maximum of 1.18 μ_B with PBE in VASP. The moments on Fe atoms are high in Pt-rich clusters and decrease as the number of Fe atoms in the core increases as well as the size of the cluster increases. From Bader charge analysis, the charge on Fe atoms is depleted by about 0.7 e, while the charge on Pt is in excess by about 0.5 e, indicating significant charge transfer from Fe to Pt atoms. This behavior is similar to that in bulk Fe-Pt alloys. The charge transfer from Fe atoms can also lead to an enhancement in the magnetic moments as some of the down spin states become unoccupied as in Fe_4Pt, but there is also hybridization between Fe 3d and Pt 5d states. This can also lead to a reduction in the magnetic moments on Fe atoms as in Fe_6Pt in spite of the charge transfer. This shows that the magnetic moments of Fe atoms after interaction with Pt atoms do not necessarily increase and it may depend on the cluster size, number of Fe and Pt atoms, their distribution, and the atomic structure.

The charge transfer and change in magnetic moments are generally between those Fe and Pt atoms that interact directly. Therefore, these effects are local in nature. The densities of states of Fe-Pt clusters are dominated by the d states of Fe and Pt atoms with the HOMO and LUMO having strong contribution from Fe 3d states. The calculated lowest harmonic frequencies for all structural isomers are found to be positive which suggests the dynamical stability of the obtained structures. We also calculated the electric dipole moments on the lowest energy isomers and all these results would help to establish the structure and properties of these clusters from experiments. We expect that our results would have strong bearing on the understanding of the catalytic behavior of these clusters as well as help to understand the behavior of larger clusters. We also hope that our results would stimulate experiments on mass abundance as well as measurements of the magnetic moments, electric dipole moments, IR and Raman spectra, as well as photoelectron spectroscopy on these small clusters that would further help to confirm the results presented here.

ACKNOWLEDGMENTS

We are thankful to the staff of the Centre for Development of Advanced Computing (C-DAC) for providing the supercomputing resources and their excellent support. We also thank Dr. Amol B. Rahane and Dr. Arpan K. Deb for some help in computations. Financial support from the Asian Office of Aerospace Research and Development (AOARD) under project Grant No. FA2386-13-1-4034 is gratefully acknowledged.

[1] R. Ferrando, J. Jellinek, and R. L. Johnston, Nanoalloys: From theory to applications of alloy clusters and nanoparticles, Chem. Rev. **108**, 845 (2008).

[2] H. Zeng, J. Li, J. P. Liu, Z. L. Wang, and S. Sun, Exchange-coupled nanocomposite magnets by nanoparticle self-assembly, Nature (London) **420**, 395 (2002).

[3] J.-M. Qiu and J.-P. Wang, Tuning the crystal structure and magnetic properties of FePt nanomagnets, Adv. Mater. **19**, 1703 (2007).

[4] C. Wang, Y. Hou, J. Kim, and S. Sun, A general strategy for synthesizing FePt nanowires and nanorods, Angew. Chem. Int. Ed. **46**, 6333 (2007).

[5] C. Antoniak, M. E. Gruner, M. Spasova, A. V. Trunova, F. M. Römer, A. Warland, B. Krumme, K. Fauth, S. Sun, P. Entel, M. Farle, and H. Wende, A guideline for atomistic design and understanding of ultrahard nanomagnets, Nat. Commun. **2**, 528 (2011).

[6] H. Zeng, J. Li, Z. L. Wang, J. P. Liu, and S. Sun, Bimagnetic core/shell FePt/Fe_3O_4 nanoparticles, Nano. Lett. **4**, 187 (2004).

[7] S. Guo and S. Sun, FePt nanoparticles assembled on graphene as enhanced catalyst for Oxygen reduction reaction, J. Am. Chem. Soc. **134**, 2492 (2012).

[8] P. Entel, M. E. Gruner, G. Rollmann, A. Hucht, S. Sahoo, A. T. Zayak, H. C. Herper, and A. Dannenberg, First-principles investigations of multimetallic transition metal clusters, Philos. Mag. **88**, 2725 (2008).

[9] T. Miyazaki, O. Kitakami, S. Okamoto, Y. Shimada, Z. Akase, Y. Murakami, D. Shindo, Y. K. Takahashi, and K. Hono, Size effect on the ordering of $L1_0$ FePt nanoparticles, Phys. Rev. B **72**, 144419 (2005).

[10] S. Vajda, M. J. Pellin, J. P. Greeley, C. L. Marshall, L. A. Curtiss, G. A. Ballentine, J. W. Elam, S. Catillon-Mucherie, P. C. Redfern, F. Mehmood, and P. Zapol, Subnanometre platinum clusters as highly active and selective catalysts for the oxidative dehydrogenation of Propane, Nat. Mater. **8**, 213 (2009).

[11] K. Boufala, L. Fernández-Seivane, J. Ferrer, and M. Samah, Magnetic properties of Fe_{2n} and $(FePt)_n$ ($n \leqslant 5$) clusters and magnetic anisotropy of transition metal dimers, J. Magn. Magn. Mater. **322**, 3428 (2010).

[12] E. A Brandes and G. B. Brook, *Smithells Metals Reference Book, 7th ed.* (Butterworth-Heinemann, Oxford, 1992).

[13] V. Kumar, Chemical compositions at alloy surfaces, Phys. Rev. B **23**, 3756 (1981).

[14] B. Wang, D. C. Berry, Y. Chiari, and K. Barmak, Experimental measurements of the heats of formation of Fe_3Pt, FePt, and $FePt_3$ using differential scanning calorimetry, J. Appl. Phys. **110**, 013903 (2011).

[15] V. Kumar and Y. Kawazoe, Evolution of atomic and electronic structure of Pt clusters: Planar, layered, pyramidal, cage, cubic, and octahedral growth, Phys. Rev. B **77**, 205418 (2008).

[16] K. Cervantes-Salguero and J. M. Seminario, Structure and Energetics of Small Iron Clusters, J. Mol. Model. **18**, 4043 (2012).

[17] I. M. L. Billas, A. Chatelain, and W. A. de Heer, Magnetism from the atom to the bulk in Iron, Cobalt, and Nickel Clusters, Science **265**, 1682 (1994).

[18] W. Kohn and L. J. Sham, Self-consistent equations including exchange and correlation effects, Phys. Rev. **140**, A1133 (1965).

[19] G. Kresse and J. Hafner, Ab initio molecular dynamics for liquid metals, Phys. Rev. B **47**, 558 (1993).

[20] G. Kresse and J. Furthmüller, Efficient iterative schemes for Ab initio total-energy calculations using a plane-wave basis set, Phys. Rev. B **54**, 11169 (1996).

[21] P. E. Blöchl, Projector augmented-wave method, Phys. Rev. B **50**, 17953 (1994).

[22] G. Kresse and D. Joubert, From ultrasoft pseudopotentials to the projector augmented-wave method, Phys. Rev. B **59**, 1758 (1999).

[23] J. P. Perdew, K. Burke, and M. Ernzerhof, Generalized Gradient Approximation Made Simple, Phys. Rev. Lett. **77**, 3865 (1996).

[24] H. Purdum, P. A. Montano, G. K. Shenoy, and T. Morrison, Extended x-ray absorption fine structure study of small Fe molecules isolated in solid neon, Phys. Rev. B **25**, 4412 (1982).

[25] L. Lian, C. X. Su, and P. B. Armentrout, Collision induced dissociation of Fe_n^+(n = 2 − 19) with Xe: Bond energies, geometric structures, and dissociation pathways, J. Chem. Phys. **97**, 4072 (1992).

[26] M. Moskovits and D. P. Di-Lella, Di-iron and nickeliron, J. Chem. Phys. **73**, 4917 (1980).

[27] J. Paier, R. Hirschl, M. Marsman, and G. Kresse, The Perdew-Burke ernzerhof exchange-correlation functional applied to the G2-1 test set using a plane-wave basis set, J. Chem. Phys. **122**, 234102 (2005).

[28] A. V. Krukau, O. A. Vydrov, A. F. Izmaylov, and G. E. Scuseria, Influence of the exchange screening parameter on the performance of screened Hybrid functionals, J. Chem. Phys. **125**, 224106 (2006).

[29] G. Rollmann, H. C. Herper, and P. Entel, Electron correlation effects in the Fe dimer, J. Phys. Chem. A **110**, 10799 (2006).

[30] H. J. Kulik, M. Cococcioni, D. A. Scherlis, and N. Marzari, Density Functional Theory in Transition-Metal Chemistry: A Self-consistent Hubbard U approach, Phys. Rev. Lett. **97**, 103001 (2006).

[31] Y. R. Jang and B. D. Yu, Structural, magnetic, and electronic properties of Fe: A screened Hybrid functional study, J. Magn. **16**, 201 (2011).

[32] M. J. Frisch *et al.*, GAUSSIAN09, Revision D.01, Gaussian, Inc., Wallingford CT (2013).

[33] F. A. Hamprecht, A. J. Cohen, D. J. Tozer, and N. C. Handy, Development and assessment of new exchange-correlation functionals, J. Chem. Phys. **109**, 6264 (1998).

[34] A. D. Boese, N. L. Doltsins, N. C. Handy, and M. Sprik, New generalized gradient approximation functionals, J. Chem. Phys. **112**, 1670 (2000).

[35] A. D. Boese and N. C. Handy, A new parametrization of exchange correlation generalized gradient approximation functionals, J. Chem. Phys. **114**, 5497 (2001).

[36] P. J. Hay and W. R. Wadt, Ab initio effective core potentials for molecular calculations: Potentials for the transition metal atoms Sc to Hg, J. Chem. Phys. **82**, 270 (1985).

[37] W. R. Wadt and P. J. Hay, Ab initio effective core potentials for molecular calculations: Potentials for main group elements Na to Bi, J. Chem. Phys. **82**, 284 (1985).

[38] P. J. Hay and W. R. Wadt, Ab initio effective core potentials for molecular calculations: Potentials for K to Au including the outermost core orbitals, J. Chem. Phys. **82**, 299 (1985).

[39] See Supplemental Material at http://link.aps.org/supplemental/10.1103/PhysRevB.92.125442 for comparison of the binding energy (BE) of Fe_2, Pt_2, FePt, Fe_2Pt_2, Fe_4Pt_4, and Fe_4Pt_6 calculated using the methods PBE, PBE0, HSE06 in VASP and HCTH/LANL2DZ in GAUSSIAN09 program (Table S1). Figure S1 shows the BE of pure Fe and pure Pt clusters using different exchange-correlation functional. Also, the BE, dipole moment, second order difference of the total energy (Δ_2), and heat of formation (ΔH) per atom of Fe_mPt_n ($m + n = 2 - 10$) clusters calculated using the methods HCTH/LANL2DZ in GAUSSIAN09 and PBE in VASP are given in Tables S2 and S3 along with the optimized lowest energy isomers using the PBE method. The magnetic moments on Fe atoms in different nanoalloys are given in Fig. S2. The excess and depletion of charge for selected Fe-Pt clusters are given in Fig. S3. Table S4 gives the optimized structures of the lowest energy isomers along with the atom number using the PBE method. The total magnetic moments (μ_B) for the lowest energy isomers, charge and local magnetic moments (μ_B) on Fe and Pt atoms in each isomer, and the number of first nearest neighbour (γ) for each atom of Fe_mPt_n ($m + n = 2 - 10$) clusters are given in Tables S5–S9. The spin-polarized total and angular momentum decomposed partial densities of states for the lowest energy isomers of FePt, Fe_2Pt_2, Fe_4Pt_4, and Fe_4Pt_6 clusters are given on Figs. S4 and S5 using the PBE method in VASP. The IR and Raman spectra calculated from HCTH/LANL2DZ for Fe_N and Pt_N ($N = 3 - 10$) clusters are given in Fig. S6. The vibrational frequencies along with infrared intensity and Raman activity of Fe_mPt_n ($m + n = 2 - 10$) clusters obtained by using HCTH/LANL2DZ method are given in Tables S10–S14.

[40] M. Niemeyer, K. Hirsch, V. Zamudio-Bayer, A. Langenberg, M. Vogel, M. Kossick, C. Ebrecht, K. Egashira, A. Terasaki, T. Möller, B. v. Issendorff, and J. T. Lau, Spin Coupling and Orbital Angular Momentum Quenching in Free Iron Clusters, Phys. Rev. Lett. **108**, 057201 (2012).

[41] K. E. Andersen, V. Kumar, Y. Kawazoe, and W. E. Pickett, Origin of Spontaneous Electric Dipoles in Homonuclear Niobium Clusters, Phys. Rev. Lett. **93**, 246105 (2004).

[42] K. E. Andersen, V. Kumar, Y. Kawazoe, and W. E. Pickett, Origin and temperature dependence of the electric dipole moment in niobium clusters, Phys. Rev. B **73**, 125418 (2006).

[43] B. L. Chittari and V. Kumar, Ab initio studies of segregation, ordering, and magnetic behavior in $(FePt)_n$, $n = 55$ and 147: Design of $Fe_{75}Pt_{72}$ nanoparticle, J. Phys. Chem. C **119**, 11062 (2015).